HHS Public Access

Author manuscript

Cell Host Microbe. Author manuscript; available in PMC 2022 July 31.

Published in final edited form as:

Cell Host Microbe. 2020 November 11; 28(5): 683–698.e6. doi:10.1016/j.chom.2020.07.019.

Legionella-infected macrophages engage the alveolar epithelium to metabolically reprogram myeloid cells and promote antibacterial inflammation

Xin Liu[1], **Mark A. Boyer**[1], **Alicia M. Holmgren**[1,2], **Sunny Shin**[1,3,*]

[1]Department of Microbiology, Perelman School of Medicine, University of Pennsylvania, Philadelphia, PA, 19104, USA

[2]Current address: Department of Biological Sciences, University of Alaska, Anchorage, AK, 99508, USA

[3]Lead Contact

Summary

Alveolar macrophages are among the first immune cells that respond to inhaled pathogens. However, numerous pathogens block macrophage-intrinsic immune responses, making it unclear how robust antimicrobial responses are generated. The intracellular bacterium *Legionella pneumophila* inhibits host translation, thereby impairing cytokine production by infected macrophages. Nevertheless, *Legionella*-infected macrophages induce an IL-1-dependent inflammatory cytokine response by recruited monocytes and other cells that controls infection. How IL-1 directs these cells to produce inflammatory cytokines is unknown. Here, we show that collaboration with the alveolar epithelium is critical for controlling infection. IL-1 induces the alveolar epithelium to produce granulocyte-macrophage colony-stimulating factor (GM-CSF). Intriguingly, GM-CSF signaling amplifies inflammatory cytokine production in recruited monocytes by enhancing TLR-induced glycolysis. Our findings reveal that alveolar macrophages engage alveolar epithelial signals to metabolically reprogram monocytes for antibacterial inflammation.

eTOC Blurb

Xin et al. show that the alveolar epithelium enables communication between infected alveolar macrophages and recruited myeloid cells during pulmonary bacterial infection. Mechanistically, IL-1 released by infected macrophages induces the alveolar epithelium to produce GM-CSF.

*Corresponding author: sunshin@pennmedicine.upenn.edu.

Author Contributions

X.L., A.M.H, and S.S. conceived and designed experiments. X.L., M.A.B., and A.M.H. performed experiments. X.L., M.A.B., A.M.H., and S.S. analyzed and interpreted data. X.L. prepared figures. X.L. and S.S. wrote the paper.

Declaration of Interests

The authors declare no competing interests.

GM-CSF in turn metabolically reprograms monocytes, amplifying inflammatory responses and promoting host defense.

Graphical Abstract

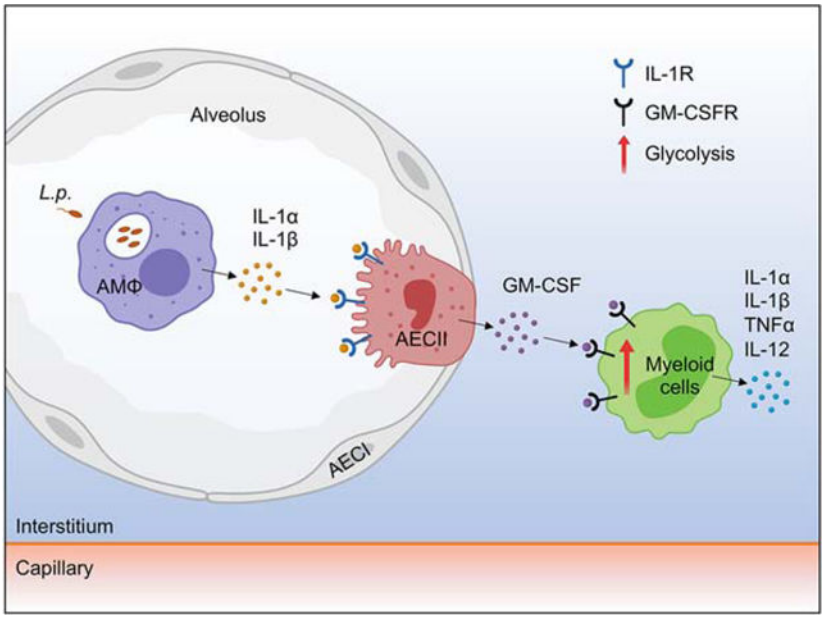

Keywords

Legionella ; innate immunity; IL-1R; alveolar epithelium; GM-CSF; macrophages; monocytes; immunometabolism

Introduction

The lung is one of the largest mucosal surfaces in the body, with the alveolar compartment representing the majority of the epithelial surface within the lung. Alveolar macrophages are the primary immune cells present in the alveoli and are key cellular sensors of pathogens. Antimicrobial immunity by alveolar macrophages is thought to be initiated upon sensing of pathogen-associated molecular patterns (PAMPs) by pattern recognition receptors (PRRs). Subsequently, there is recruitment of bystander myeloid cells, such as monocytes (MCs) and neutrophils, which amplify inflammatory responses important for controlling infection (Chaplin, 2010; Iwasaki and Medzhitov, 2015). However, only one alveolar macrophage patrols every three alveoli (Bhattacharya and Westphalen, 2016; Westphalen et al., 2014), and it is unclear how a limited number of macrophages can defend such a vast surface area. In addition, numerous pathogens disarm alveolar macrophages by deploying virulence factors that impair cell-intrinsic PRR signaling. Thus, how a robust antimicrobial response is generated against respiratory pathogens remains a fundamental question.

To define how antimicrobial immunity is generated in response to pathogens that interfere with immune signaling, we utilized *Legionella pneumophila,* which causes the severe

pneumonia Legionnaires' disease (Fraser et al., 1977; McDade et al., 1977). *Legionella* infects and replicates within alveolar macrophages (Copenhaver et al., 2014). To do so, *Legionella* employs a bacterial type IV secretion system (T4SS) to translocate effector proteins into the host cell (Isberg et al., 2009; Nagai and Kubori, 2011; Sherwood and Roy, 2016). These effectors manipulate numerous host processes to promote bacterial replication within macrophages (Isberg et al., 2009; Qiu and Luo, 2017; Sherwood and Roy, 2016). A subset of these effectors potently inhibit host translation (Barry et al., 2013; Belyi et al., 2008; De Leon et al., 2017; Fontana et al., 2011; Moss et al., 2019; Shen et al., 2009). As a result, infected macrophages are incapable of making cytokines, such as TNF and IL-12 (Copenhaver et al., 2015), which are required to control infection (Brieland et al., 1998; Skerrett et al., 1997). However, infected cells still translate IL-1α and IL-1β and undergo inflammasome-dependent cytokine release (Asrat et al., 2014; Barry et al., 2017; Copenhaver et al., 2015). Critically, IL-1R signaling instructs bystander recruited myeloid cells to produce inflammatory cytokines and control of infection (Copenhaver et al., 2015). These findings indicate that IL-1 released initially by *Legionella*-infected macrophages drives the production of critical cytokines by bystander cells, allowing for immune bypass of the bacterial block in host translation to enable control of infection.

IL-1R signaling is important for control of *Legionella* and many other microbial infections, but how IL-1 instructs bystander cytokine responses is poorly understood. IL-1R is expressed by both hematopoietic and non-hematopoietic cells (Cunningham et al., 1992; Dinarello, 1998; Ueda et al., 2009). Whether cell-intrinsic IL-1R signaling instructs myeloid cells to produce cytokines *in vivo* is unknown. Here, we report that IL-1R signaling on alveolar type II epithelial cells (AECII), rather than immune cells, was critical in driving cytokine production by Ly6C^{hi} MCs and CD11b^{+} dendritic cells (DCs) and control of *Legionella* infection. Mechanistically, IL-1 was necessary to instruct AECII to make the cytokine GM-CSF, which in turn promoted production of inflammatory cytokines by Ly6C^{hi} MCs and CD11b^{+} DCs recruited to the lung. Intriguingly, GM-CSF metabolically reprogrammed MCs to undergo heightened aerobic glycolysis, which was required for robust cytokine expression. This study provides new insight into the role of the alveolar epithelium as a central signal relay between infected alveolar macrophages and recruited MCs via an IL-1/GM-CSF circuit, which metabolically reprograms MCs to promote antibacterial inflammation and host defense.

Results

Non-hematopoietic IL-1R signaling instructs Ly6C^{hi} MCs and CD11b^{+} DCs to produce inflammatory cytokines and control of infection

IL-1R is expressed by both hematopoietic and stromal cells in the lung, raising the question of which cell types respond to IL-1 to enable inflammatory responses during *Legionella* infection. We generated bone marrow (BM) chimeras in which IL-1R expression was confined to the stromal compartment by providing *Il1r1*$^{-/-}$ BM to lethally irradiated WT mice (*Il1r1*$^{-/-}$→WT) or the hematopoietic compartment by providing WT BM to lethally irradiated *Il1r1*$^{-/-}$ mice (WT→*Il1r1*$^{-/-}$), along with control chimeras (WT→WT or *Il1r1*$^{-/-}$→*Il1r1*$^{-/-}$). Following hematopoietic reconstitution (Figure S1A), we intranasally

infected the chimeras with a sublethal dose of *Legionella.* As flagellin delivered by the T4SS into the host cell cytosol induces rapid cell death due to NAIP5 inflammasome activation, we used flagellin-deficient (Δ*flaA*) *Legionella* for our studies. Δ*flaA Legionella* evade NAIP5 detection and replicate in C57BL/6J macrophages and mice (Molofsky et al., 2006; Ren et al., 2006; Zamboni et al., 2006), but still induce NLRP3 and caspase-11 inflammasome activation and IL-1 family cytokine secretion (Case et al., 2013; Casson et al., 2013). Following infection, we assessed cytokine production in the bronchoalveolar lavage (BAL) at 24 hours post-infection (hpi). Mice lacking stromal IL-1R expression had a significant defect in TNF, IL-12, and IL-6 production compared to WT→WT or *Il1r1*$^{-/-}$→WT mice (Figure 1A). Ly6C^{hi} MCs and MC-derived DCs are major producers of inflammatory cytokines such as TNF and IL12 during *Legionella* infection (Brown et al., 2016; Casson et al., 2017). We observed that both the frequency and total number of TNF- or IL-12-producing Ly6C^{hi} MCs and conventional DCs (cDCs) in the lung were significantly reduced in WT→*Il1r1*$^{-/-}$ mice (Figure 1B and Figure S1B), although total numbers of Ly6C^{hi} MCs and cDCs in the different chimeras were equivalent (Figure S1C). Indeed, the observed cytokine defect in WT→*Il1r1*$^{-/-}$ mice was indistinguishable from *Il1r1*$^{-/-}$→*Il1r1*$^{-/-}$ mice. These data indicate that stromal IL-1R signaling was required for MCs and cDCs to produce inflammatory cytokines during infection.

In contrast, both stromal and hematopoietic IL-1R signaling was necessary for CXCL1 production and neutrophil recruitment, although loss of stromal IL-1R signaling had a greater impact (Figure 1C and 1D). At 24 hpi, bacterial loads were equivalent in all chimeras (Figure S1D), indicating that decreased cytokine production in mice lacking stromal IL-1R signaling was not due to elevated levels of bacteria inhibiting protein synthesis. Critically, loss of stromal IL-1R expression was associated with failure to control bacterial burden later during infection, as WT→*Il1r1*$^{-/-}$ and *Il1r1*$^{-/-}$→*Il1r1*$^{-/-}$ mice had significantly higher bacterial loads compared to WT→WT and *Il1r1*$^{-/-}$→WT mice at 72 hpi (Figure 1E). Collectively, these data indicate that IL-1R signaling within stromal cells, but not hematopoietic cells, is required for MCs- and cDCs-derived inflammatory cytokine production and control of infection.

IL-1R on alveolar type II epithelial cells is essential for inflammatory cytokine production and antibacterial defense

Within the alveoli, alveolar type II epithelial cells (AECII) are a major stromal cell type that constitute 60% of alveolar epithelial cells (Crapo et al., 1982) and express IL-1R (Blau et al., 1994; Thorley et al., 2007). To test whether IL-1R expression on AECII is required for inflammatory cytokine production and control of bacterial infection, we generated mice lacking IL-1R on AECII by crossing *Il1r1*$^{fl/fl}$ mice with mice expressing tamoxifen (TXF)-inducible CreER^{T2} under the control of the AECII-specific surfactant protein C promoter (*Spc-creER*^{T2}) (Rock et al., 2011). Following infection, TXF-treated *Il1r1*$^{fl/fl}$;*Spc-creER*^{T2} mice exhibited significantly lower TNF, IL-12, and IL-6 production (Figure 2A). These mice also had a log increase in lung bacterial loads compared to *Il1r1*$^{fl/fl}$ mice, whereas in the absence of TXF treatment, *Il1r1*$^{fl/fl}$;*Spc-creER*^{T2} and *Il1r1*$^{fl/fl}$ mice had similar bacterial loads (Figure 2B). TXF treatment resulted in ~80% deletion of the *Il1r1* locus in AECII from *Il1r1*$^{fl/fl}$;*Spc-creER*^{T2} mice compared to *Il1r1*$^{fl/fl}$ mice (Figure

2C). Further, to test whether IL-1R expression on AECII alone can mediate inflammatory cytokine responses and control of infection, we limited IL-1R expression largely to AECII by crossing *Spc-creER^{T2}* mice with *Il1r1$^{r/r}$* mice. In these mice, the *Il1r1* gene is disrupted by a loxP-flanked interfering sequence that prevents transcription or translation of *Il1r1* prior to Cre recombinase exposure and contains an IRES-tdTomato reporter to track *Il1r1* mRNA expression (Liu et al., 2015). Strikingly, TXF-treated *Il1r1$^{r/r}$*;*Spc-creER^{T2}* mice exhibited significant restoration of TNF, IL-12, and IL-6 production and decreased bacterial loads compared to *Il1r1$^{r/r}$* mice (Figure 2D and 2E). Approximately 60% of AECII were tdTomato-positive; by contrast, a small percentage of other stromal lung cells, including alveolar type I epithelial cells (AECI) and bronchial alveolar stem cells (BASC), were tdTomato-positive, indicating that IL-1R expression was predominantly restored in AECII (Figure 2F), whereas AECII from TXF-treated *Il1r1$^{r/r}$* mice did not express tdTomato. Altogether, these results indicate that IL-1R signaling in AECII is indispensable for driving inflammatory cytokine responses and bacterial clearance.

IL-1R signaling in AECII drives production of GM-CSF

We hypothesized that IL-1R signaling in AECII induces production of a soluble mediator that licenses recruited myeloid cells to produce inflammatory cytokines. We therefore analyzed the BAL of WT and *Il1r1$^{-/-}$* mice at 24 hpi using a Luminex assay to identify soluble factors that required IL-1R signaling for their induction. Many cytokines were reduced in the BAL of *Il1r1$^{-/-}$* mice compared to WT mice (Figure S2A). Interestingly, GM-CSF production was also reduced in the BAL of *Il1r1$^{-/-}$* mice. GM-CSF was initially described as a hematopoietic growth factor and is often used to promote DC differentiation from mouse hematopoietic progenitors *in vitro* (Inaba et al., 1992). However, at steady state in mice, GM-CSF is mostly dispensable for the development of myeloid cells, except for a slight reduction in some DC populations and the absence of alveolar macrophages (Bogunovic et al., 2009; Dranoff et al., 1994; Greter et al., 2012; Guilliams et al., 2013; Shibata et al., 2001; Stanley et al., 1994). Intriguingly, GM-CSF can be robustly induced and acts as a cytokine that elicits myeloid cell responses in various inflammatory settings (Anzai et al., 2017; Becher et al., 2016; Croxford et al., 2015; Tugues et al., 2018). Furthermore, GM-CSF is required for host defense against several lung pathogens, such as *Mycobacterium tuberculosis, Aspergillus fumigatus, Blastomyces dermatitidis,* and influenza virus (Hernandez-Santos et al., 2018; Huang et al., 2011; Kasahara et al., 2016; Rothchild et al., 2014). In these settings, it is thought that GM-CSF enhances the killing activity of alveolar macrophages and neutrophils; however, precisely how GM-CSF mediates host defense is poorly understood. We therefore considered the possibility that GM-CSF may synergize with other inflammatory signals to enhance anti-bacterial cytokine responses. Following *Legionella* infection, GM-CSF was robustly induced in the lungs by 24 hours, and declined to background levels by 72 hours (Figure 3A). Critically, GM-CSF levels were nearly undetectable in *Il1a$^{-/-}$*, *Il1b$^{-/-}$*, or *Il1r1$^{-/-}$* mice at 24 hpi (Figure 3B), indicating that IL-1R signaling is required for GM-CSF production during infection.

GM-CSF is produced by a variety of cell types, including lymphocytes, macrophages, fibroblasts, and endothelial cells, in response to immune stimuli (Cousins et al., 1994; Nimer and Uchida, 1995; Ponomarev et al., 2007; Sonderegger et al., 2008). Under steady state

conditions, GM-CSF is produced by lung epithelial cells (Guilliams et al., 2013; Huffman et al., 1996; Schneider et al., 2014). To determine whether a hematopoietic or stromal cell type produced GM-CSF during *Legionella* infection, we generated BM chimeras in which GM-CSF expression was confined to stromal cells (*Csf2*$^{-/-}$→WT), or to hematopoietic cells (WT→*Csf2*$^{-/-}$), and control chimeras (WT→WT and *Csf2*$^{-/-}$→*Csf2*$^{-/-}$). *Csf2*$^{-/-}$→WT mice produced GM-CSF at levels similar to WT→WT mice following infection, whereas GM-CSF was undetectable in mice lacking stromal GM-CSF (Figure 3C). Moreover, following infection, *Csf2* transcript levels were the highest in AECII relative to other lung cell types (Figure 3D), and the frequency and total number of GM-CSF-producing AECII significantly increased, whereas AECI were unchanged (Figure 3E). These data indicate that AECII are the primary source of GM-CSF early during infection.

We next asked whether GM-CSF production requires IL-1R signaling in AECII. Critically, WT→*Il1r1*$^{-/-}$ BM chimeras lacking stromal IL-1R expression or *Il1r1*$^{fl/fl}$;*Spc-creER*^{T2} mice lacking IL-1R in AECII had a significant defect in GM-CSF production compared to WT→WT chimeras or *Il1r1*$^{fl/fl}$ mice, respectively, following infection (Figure 3F and 3G). Consistently, GM-CSF production was restored in *Il1r1*$^{r/r}$;*Spc-creER*^{T2} mice expressing IL-1R mainly on AECII compared to *Il1r1*$^{r/r}$ mice lacking IL-1R signaling (Figure 3H). Furthermore, recombinant IL-1 (rIL-1α/β) induced GM-CSF in purified WT AECII but not in *Il1r1*$^{-/-}$ AECII during *in vitro Legionella* infection (Figure 3I). These results indicate that GM-CSF is predominantly produced by AECII in response to IL-1 during *Legionella* infection.

GM-CSF is critical for local inflammatory cytokine production by MCs and bacterial clearance

We hypothesized that AECII production of GM-CSF is critical for recruited immune cells to produce inflammatory cytokines important for bacterial clearance. In support of this model, *Csf2*$^{-/-}$ mice had significant defects in producing IL-1β and TNF at 24 hpi and TNF, IL-12, and IFNγ at 48 hpi (Figure 4A), and a log increase in bacterial loads at 72 hpi compared to WT mice (Figure 4B). To address the possibility that these effects could be due to a lack of alveolar macrophages in *Csf2*$^{-/-}$ mice due to the critical role for GM-CSF in alveolar macrophage development, we acutely blocked GM-CSF with neutralizing antibodies, as this treatment leaves the alveolar macrophage compartment intact (Figure S3A). Notably, GM-CSF blockade led to significantly decreased IL-1β levels at 24 hour post-infection and TNF, IL-12, and IFNγ levels at 48 hour post-infection (Figure 4C), and a log increase in bacterial loads at 72 hpi compared to isotype control-treated mice (Figure 4D). The frequency and total number of IL-1β- or IL-1α-producing MCs were significantly reduced as well (Figure 4E and Figure S3B). Importantly, these effects of GM-CSF deficiency were independent of its growth factor properties, as numbers of neutrophils, MCs, and DCs in the lungs of anti-GM-CSF-treated mice were largely unaffected (Figure S3C). Collectively, these data demonstrate that GM-CSF is required for cytokine responses and bacterial clearance.

We next asked whether GM-CSF enhances cytokine production by MCs distally within the systemic circulation (peripheral blood MCs) or locally within the lung. We injected mice intravenously with anti-CD45-PE antibodies to label all circulating immune cells, followed

by staining of all lung cells with antiCD45-Alexa Fluor 488 antibodies to distinguish MCs circulating within or adhered to the pulmonary vasculature (vascular MCs) from MCs that entered the lung interstitium (interstitial MCs). The numbers of interstitial and vascular MCs within the lungs of infected mice were significantly increased compared to naïve mice (Figure 4F). Antibody-mediated blockade of GM-CSF in infected mice significantly decreased the frequency and total number of IL-1-producing interstitial and vascular MCs within the lung compared to isotype control-treated mice (Figure 4G and Figure S3D). In contrast, there were substantially lower numbers of IL-1-producing peripheral blood MCs compared to lung MCs, with no difference in the numbers of IL-1-producing peripheral blood MCs in anti-GM-CSF- or isotype control-treated mice (Figure 4G and Figure S3D). These data indicate that GM-CSF has a potent local effect by licensing MCs within the lung environment to produce inflammatory cytokines during infection.

We next sought to determine whether GM-CSF controls *Legionella* infection by inducing inflammatory cytokines or by promoting other antimicrobial effector functions. As GM-CSF blockade led to a defect in IL-12 production (Figure 4C), and IL-12 is critical for control of *Legionella* (Brieland et al., 1998), we tested the hypothesis that IL-12 was a downstream mediator of GM-CSF-dependent bacterial clearance. Administering recombinant IL-12 p70 to anti-GM-CSF-treated mice significantly reduced bacterial loads down to levels similar to those in isotype control-treated mice (Figure 4H). Although GM-CSF treatment of macrophages can inhibit intracellular *M. tuberculosis* replication (Rothchild et al., 2014), we observed no significant difference in *Legionella* replication within WT and *Csf2*$^{-/-}$ BM-derived macrophages (BMDMs), or BMDMs treated with rGM-CSF (Figure S3E). GM-CSF can promote reactive oxygen species (ROS) production in neutrophils during *A. fumigatus* infection (Kasahara et al., 2016), but we did not observe decreased neutrophil ROS production in the lungs of anti-GM-CSF-treated mice compared to isotype control-treated mice during *Legionella* infection (Figure S3F). Collectively, these data indicate that AECII-derived GM-CSF mediates bacterial clearance primarily by promoting production of inflammatory cytokines such as IL-12 by immune cells.

Myeloid cell-intrinsic GM-CSF receptor signaling controls inflammatory cytokine production

GM-CSF could instruct Ly6C^{hi} MCs and CD11b^{+} DCs to produce inflammatory cytokines directly, or through yet another intermediary signal. We next asked whether myeloid cell-intrinsic GM-CSF signaling was required for cytokine production. We generated BM chimeric mice in which GM-CSF receptor expression was absent from hematopoietic cells (*Csf2rb*$^{-/-}$→WT), or mixed BM chimeras in which lethally irradiated WT mice were reconstituted with a 1:1 mixture of congenically marked WT and *Csf2rb*$^{-/-}$ BM (Figure S4A). Notably, consistent with our previous findings with GM-CSF deficiency, there were significantly decreased IL-1α, IL-1β, TNF, IL-12, IL-6, and IFNγ levels in the BAL of *Csf2rb*$^{-/-}$→WT mice compared to WT→WT or mixed BM chimeras following *Legionella* infection (Figure 5A). Moreover, the frequency and total number of IL-1-producing MCs and cDCs were significantly reduced in *Csf2rb*$^{-/-}$→WT mice compared to WT→WT mice (Figure 5B and S4B), although there was no difference in total MC numbers and only a slight reduction in cDCs (Figure S4C). *Csf2rb*$^{-/-}$→WT mice also exhibited a log increase

in bacterial loads compared to WT→WT mice (Figure 5C), indicating a crucial role for hematopoietic GM-CSF receptor signaling in inflammatory cytokine production and control of infection.

Critically, in mixed BM chimeras, the presence of WT cells was unable to rescue cytokine production by *Csf2rb*$^{-/-}$ cells, as the frequency of IL-1-producing *Csf2rb*$^{-/-}$ MCs and cDCs was significantly reduced relative to WT cells within the same mouse (Figure 5D and S4D). Moreover, *Il1a, Il1b, Tnf, Il6,* and *Il12a* transcript levels were significantly reduced in *Csf2rb*$^{-/-}$ Ly6C^{hi} MCs and Ly6C^{+} inflammatory DCs (iDCs), compared to WT cells within the same mouse (Figure 5E and Figure S4E). Collectively, these data indicate that Ly6C^{hi} MCs- and iDCs-intrinsic GM-CSF receptor signaling is critical for inflammatory cytokine gene expression following infection.

GM-CSF enhances inflammatory cytokine expression in a JAK2/STAT5-dependent manner

We next sought to understand how GM-CSF receptor signaling regulates cytokine production. Consistent with our *in vivo* observations, addition of rGM-CSF to isolated MCs infected with *Legionella ex vivo* increased IL-1α, IL-1β, TNF, and IL-12 protein and mRNA levels compared to PBS vehicle control (Figure 6A and 6B). We next investigated whether GM-CSF-mediated enhancement of cytokine responses in MCs was specific to infection with virulent *Legionella* expressing a T4SS. To do so, avirulent Δ*dotA Legionella* lacking a functional T4SS (Berger and Isberg, 1993; Roy et al., 1998; Vogel et al., 1998) or *E. coli*-derived LPS was used. Addition of rGM-CSF to *ΔdotA Legionella*-infected or *E. coli* LPS-treated MCs led to increased *Il1a*, *Il1b*, *Tnf,* and *Il12a* mRNA levels and TNF and IL-12 protein levels compared to PBS (Figure S5A), suggesting that GM-CSF enhances cytokine production in response to PAMPs as well. MCs infected with *ΔdotA Legionella* failed to secrete IL-1α and IL-1β regardless of rGM-CSF or PBS treatment (Figure S5B), indicating that IL-1 cytokine secretion by MCs is T4SS-dependent.

GM-CSF receptor signaling leads to JAK2 activation and subsequent phosphorylation of the transcription factor STAT5 (Mui et al., 1995; Quelle et al., 1994). We observed that treatment with the JAK2 inhibitor NVP-BSK805 and the STAT5 inhibitor Pimozide reduced *Il1a, Il1b, Tnf,* and *Il12a* transcript levels in MCs in a dose-dependent manner following rGM-CSF treatment and *Legionella* infection (Figure 6C and 6D). These data indicate that GM-CSF-dependent JAK2/STAT5 signaling plays an important role in inducing inflammatory cytokine expression during infection.

GM-CSF-enhanced glycolytic activity is required for inflammatory cytokine production by MCs

TLR activation results in increased glycolytic capacity of myeloid cells, and aerobic glycolysis is required for TLR-dependent expression of inflammatory genes (Everts et al., 2014; Krawczyk et al., 2010; Langston et al., 2017; Mills et al., 2016; Rodriguez-Prados et al., 2010; Tannahill et al., 2013). Intriguingly, GM-CSF enhances LPS-induced glycolysis in BMDMs (Na et al., 2016). We thus hypothesized that GM-CSF promotes glycolytic reprogramming of MCs, and that this enhanced glycolysis contributes to inflammatory gene expression during *Legionella* infection.

We first asked whether GM-CSF causes metabolic alterations in MCs by measuring glycolysis and mitochondrial oxidative phosphorylation through analysis of the extracellular acidification rate (ECAR) and oxygen consumption rate (OCR), respectively. *Legionella* infection or LPS treatment of purified MCs *ex vivo* led to increased glycolysis and glycolytic capacity over uninfected MCs (Figure 7A and 7B). Addition of rGM-CSF led to even greater increases in glycolytic activity compared to MCs incubated with *Legionella* or LPS alone (Figure 7A and 7B). In contrast, rGM-CSF treatment did not alter mitochondrial respiration in response to *Legionella* or LPS (Figure S6A and S6B). Furthermore, the rGM-CSF-mediated increase in glycolysis was blocked by pharmacological inhibition of JAK2 or STAT5 (Figure S6C and S6D). These data indicate that the GM-CSF/JAK2/STAT5 axis promotes glycolytic reprogramming of MCs.

We next sought to understand how GM-CSF enhances glycolytic activity in MCs. We examined whether GM-CSF induces expression of glycolysis-related genes. Indeed, we found that addition of rGM-CSF to uninfected, *Legionella*-infected, or LPS-treated MCs robustly increased the transcript and protein levels of key rate-limiting glycolytic genes, specifically the glucose transporter *Glut1*, hexokinase *Hk2,* and phosphofructokinase *Pfkp,* but not of other glycolysis-related genes, compared to MCs treated with PBS (Figure 7C-E). Addition of rGM-CSF to LPS- or *Legionella*-treated MCs also increased pro-IL-1β protein levels (Figure 7E). Moreover, GM-CSF-mediated upregulation of *Glut1*, *Hk2*, and *Pfkp* was blocked by pharmacological inhibition of JAK2 or STAT5 (Figure S6E). We next investigated whether GM-CSF signaling promotes expression of glycolysis-related genes *in vivo* by examining WT and *Csf2rb*$^{-/-}$ MCs from mixed BM chimeras. *Csf2rb*$^{-/-}$ MCs had a significant defect in the expression of *Glut1*, *Hk2*, *Pfkp* (Figure 7F), as well as *Gapdh* and *Eno1* (Figure S6F), but not of other glycolysis-related genes, relative to WT MCs from the same mouse during *Legionella* infection. These data suggest that GM-CSF reprograms MCs for increased glycolysis by upregulating *Glut1*, *Hk2*, and *Pfkp* expression.

We next tested whether GM-CSF-mediated glycolytic reprogramming of MCs promotes inflammatory cytokine production during *Legionella* infection. Treatment of MCs with 2-Deoxy-D-glucose (2-DG), a synthetic glucose analog often used to block glycolysis (Wick et al., 1957), significantly suppressed rGM-CSF-dependent induction of *Il1b*, *Tnf*, *and Il12a* (Figure 7G). However, 2-DG also impairs oxidative phosphorylation (Wang et al., 2018). To address whether glycolysis is specifically required for GM-CSF-dependent inflammatory gene expression, we employed media containing galactose as a sole carbon source, which must be metabolized by the Leloir pathway before entering glycolysis, resulting in a substantial reduction in glycolytic flux that effectively inhibits glycolysis (Bustamente et al., 1977; Chang et al., 2013; Weinberg et al., 2010). Incubation of MCs in galactose-only media suppressed the GM-CSF-mediated increase in glycolysis and did not alter mitochondrial respiration, compared to MCs in glucose-only media (Figure S7A and S7B). Moreover, LPS- or *Legionella*-treated MCs incubated in galactose-only media had a substantial defect in pro-IL-1β, TNF, and IL-12 production following rGM-CSF treatment compared to MCs in glucose-only media (Figure 7H and 7I). These data indicate that GM-CSF-induced glycolysis is critical for cytokine production by MCs in response to infection, as shown in the model (Figure 7J). Collectively, these results indicate that GM-CSF-dependent glycolysis and transcriptional regulation are integrated to promote

inflammatory cytokine production in MCs, thus promoting successful control of pulmonary infection.

Discussion

Within the lung, alveolar macrophages serve not only as initial sentinels of infection, but also as potential reservoirs for replication by many pulmonary pathogens. DAMPs such as IL-1, that are released from infected alveolar macrophages, have an important role as a contingency system that promotes inflammation in response to pathogens that block PRR signaling (Copenhaver et al., 2015; Pang et al., 2013). How IL-1 promotes inflammatory cytokine responses within the lung is not fully understood. Here, we show that the initially infected macrophages are insufficient on their own to direct a subsequent robust inflammatory response by recruited myeloid cells such as MCs and DCs, as IL-1 released by infected macrophages does not directly license these myeloid cells to produce inflammatory cytokines. Rather, we find that the alveolar epithelium is critical for amplifying immune responses by serving as a key signaling relay between infected alveolar macrophages and recruited myeloid cells. We found that IL-1 instructs alveolar epithelial cells to produce GM-CSF, which metabolically reprograms MCs to undergo increased glycolysis in order to support inflammatory cytokine production. GM-CSF enforces additional production of IL-1α and IL-1β by MCs, indicating that GM-CSF and IL-1 participate in a feedforward loop. Furthermore, GM-CSF is required for maximal TNF and IL-12 production and subsequent IFNγ production. TNF and IL-12 are produced primarily by uninfected bystander MCs and DCs, and MC-derived IL-12 directs IFNγ production by NK and T cells (Brown et al., 2016; Casson et al., 2017). These cytokines are required for control of *Legionella* infection (Brieland et al., 1998; Heath et al., 1996; Liu and Shin, 2019; Skerrett et al., 1997). Thus, our findings indicate that an IL-1/GM-CSF circuit is critical for amplifying inflammatory cytokine responses by bystander MCs and DCs that instruct NK and T cells to produce IFNγ, thus enabling successful control of *Legionella*.

Our findings define a three-way cell circuit initiated by release of DAMPs from infected macrophages that is relayed by the lung epithelium to license myeloid cells for maximal cytokine production. Why such an elaborate three-way communication network is necessary for amplifying cytokine responses against *Legionella* is unclear. The lung contains a surprisingly low number of alveolar macrophages, with approximately one alveolar macrophage for every three alveoli (Bhattacharya and Westphalen, 2016; Westphalen et al., 2014), indicating that a signal amplification system is needed to generate robust inflammatory responses. AECII, which comprise 60% of alveolar epithelial cells, provide a perfectly poised system to amplify the initial alarm sounded by infected macrophages in the lung. We propose that this crosstalk between the alveolar epithelium and myeloid cells allows for the robust amplification of inflammatory responses. Although such a circuit would amplify lung inflammation in the context of any microbial or foreign insult that triggers inflammasome activation and IL-1 cytokine release, it would be particularly effective in the context of immunoevasive pathogens such as *Legionella,* which interferes with host translation.

We found that GM-CSF reprogrammed MCs to undergo increased aerobic glycolysis, which was required for maximal cytokine production. Although GM-CSF was sufficient to drive glycolysis, it was not sufficient on its own to elicit cytokine production by purified MCs *ex vivo*. Instead, bacterial infection or LPS stimulation was required, suggesting that PRR sensing of PAMPs is also needed. PRRs, such as TLRs, lead to NF-κB signaling and inflammatory gene expression (Kawai and Akira, 2007). TLR-dependent TBK1 signaling also drives glycolytic reprogramming of myeloid cells that is critical for inflammatory gene expression, in part through stabilizing hypoxia-inducible factor-1α, to transcriptionally regulate *Il1b* expression, and by supporting de novo synthesis of fatty acids to allow for ER and Golgi expansion and accommodate increased protein production (Everts et al., 2014; Krawczyk et al., 2010; Mills et al., 2016; Rodriguez-Prados et al., 2010; Tannahill et al., 2013). Interestingly, we found that GM-CSF induced glycolysis and significant upregulation of the key glycolytic enzymes GLUT1, HK2, and PFKP in a JAK2/STAT5-dependent manner. In contrast, while *Legionella* or LPS alone increased glycolysis in MCs, it was not JAK2/STAT5-dependent. Thus, GM-CSF and PRR signaling likely work through distinct mechanisms to promote maximal glycolytic reprogramming of MCs. Further studies are needed to determine how GM-CSF, PRR signaling, and metabolic reprogramming collaborate for maximal inflammatory gene expression.

We found that AECII are the major producers of GM-CSF in response to IL-1 early during infection. Bronchial epithelial cells also produce GM-CSF in response to IL-1 during allergic airway responses (Willart et al., 2012). It would be of interest to determine whether in addition to IL-1, other cytokines or DAMPs also induce GM-CSF production by the lung epithelium during bacterial infection. Whether other tissues use similar mechanisms to regulate stromal GM-CSF production is unknown. In the steady-state gut, RORγt^+ innate lymphoid cells (ILCs) are the major source of GM-CSF in response to IL-1β released by macrophages upon sensing the microbiota (Mortha et al., 2014). Colonic epithelial cells produce GM-CSF in response to DSS-induced injury to promote repair of the colonic mucosa (Egea et al., 2013), and in response to invasive bacteria *in vitro* (Jung et al., 1995). Epithelial cells at other barrier tissue sites could also serve as an important source of GM-CSF by sensing IL-1 or other inflammatory mediators released in response to invasive pathogens.

It is becoming increasingly appreciated that the alveolar epithelium regulates essential immune functions during infection, such as the production of chemokines that recruit immune cells to the lung (Hernandez-Santos et al., 2018; LeibundGut-Landmann et al., 2011; Thorley et al., 2007). Our findings indicate that the alveolar epithelium also directly modifies the function of recruited MCs by reprogramming their metabolism and licensing them to produce inflammatory cytokines important for anti-bacterial defense. Understanding other signals sensed by the lung epithelium to enhance myeloid cell function may provide insight into how to modulate local inflammatory responses within the lung for the purposes of treating pulmonary infection.

STAR★Methods

RESOURCE AVAILABILITY

Lead Contact—Further information and requests for resources and reagents should be directed to and will be fulfilled by the Lead Contact, Sunny Shin (sunshin@pennmedicine.upenn.edu).

Materials Availability—This study did not generate new unique reagents.

Data and Code Availability—This study did not generate new datasets or code.

EXPERIMENTAL MODEL AND SUBJECT DETAILS

Mice—*Il1a*$^{-/-}$ and *Il1b*$^{-/-}$ (Horai et al., 1998), *Il1r1*$^{-/-}$ (Glaccum et al., 1997), *Csf2*$^{-/-}$ (Dranoff et al., 1994), *Csf2rb*$^{-/-}$ (Robb et al., 1995), *Il1r1*$^{fl/fl}$;*Spc-creER*^{T2} and *Il1r1*$^{r/r}$;*Spc-creER*^{T2} (generated by crossing *Il1r1*$^{fl/fl}$ (Robson et al., 2016) or *Il1r1*$^{r/r}$ (Liu et al., 2015) and *Spc-creER*^{T2} (Rock et al., 2011) mice in our facility) were bred and housed under specific-pathogen free conditions at the University of Pennsylvania. Wild-type C57BL/6J or B6.SJL controls or littermate controls were either purchased from Jackson Laboratories or bred in house. Mice were used at 8–10 weeks of age, gender-matched, and littermates of the same sex were randomly assigned to experimental groups. All animal studies were performed in compliance with the federal regulations set forth in the Animal Welfare Act (AWA), the recommendations in the Guide for the Care and Use of Laboratory Animals of the National Institutes of Health, and the guidelines of the University of Pennsylvania Institutional Animal Use and Care Committee. All protocols used in this study were approved by the Institutional Animal Care and Use Committee at the University of Pennsylvania (protocol #804928).

Cell lines and primary cell cultures—For generating bone marrow-derived macrophages, bone marrow cells from gender- and age-matched wild-type C57BL/6J mice and *Csf2*$^{-/-}$ mice were differentiated in RPMI supplemented with 20% FBS, 30% L929 cell supernatant, and 1% penicillin/streptomycin solution (P/S) at 37°C in a 5% CO2 incubator for 7 days. Macrophages were replated in RPMI with 10% FBS and 15% L929 cell supernatant without P/S. Primary murine monocytes were isolated from C57BL/6J bone marrow using the Monocyte Isolation Kit according to the manufacturer's instructions. Monocytes were replated in RPMI with 10% FBS without P/S. For experiments involving media containing glucose or galactose, monocytes were replated in RPMI with 10% FBS for 4 hours, and then the media was replaced with RPMI supplemented with 10% dialyzed FBS lacking glucose prior to infection and stimulation.

To isolate primary murine AECII, the lungs of gender- and age-matched WT C57BL/6J mice and *Il1r1*$^{-/-}$ mice (6–8 weeks) were perfused via the right ventricle with 5 ml PBS, lavaged with 1 ml PBS three times, inflated with a 1.5 ml mixture of 1 ml low melting agarose (3% w/v) and 500 μl 4U/ml dispase, and incubated for 1 h at room temperature (RT). The lung lobes were gently grinded on 100 μm mesh soaked in DMEM, and then filtered through 40 μm mesh. The cell suspension was centrifuged at 300 g for 10 min. The

cell pellet was resuspended in FACS buffer containing 5% FBS. AECII were then purified by fluorescence-activated cell sorting (see Experimental Details). AECII cells were plated into a Matrigel pre-coated TC plate and cultured with DMEM supplemented with charcoal-stripped 5% FBS, 10 ng/ml keratinocyte growth factor (KGF), 10 μM Rock inhibitor, and 1% P/S at 37°C in a 5% CO2 incubator for the first 2 days, and then replaced with the same media but without Rock inhibitor for the next 4 to 5 days.

Bacterial cultures—*Legionella pneumophila* JR32-derived flagellin-deficient Δ*flaA* mutant (Ren et al., 2006; Sadosky et al., 1993) and Lp02-derived (thymidine auxotroph) Δ*dotA* and Δ*flaA* mutants (Berger and Isberg, 1993; Ren et al., 2006) were cultured on charcoal yeast extract (CYE) agar plates for 48 h at 37°C prior to infection. JR32 Δ*flaA* strain was used for all *in vivo* infection and for measuring intracellular bacterial replication within BMDMs. Lp02 Δ*flaA* strain was used for all other *in vitro* experiments, with the exception of experiments in Figure S5 where Lp02 Δ*dotA* strain was used.

METHOD DETAILS

Generation of bone marrow chimeric mice—Wild-type B6.SJL mice (CD45.1 background) or knockout (KO) mice (*Il1r1*$^{-/-}$, *Csf2*$^{-/-}$, and *Csf2rb*$^{-/-}$, CD45.2 background) received a lethal dose of irradiation (1096 Rads). 6 hours later, mice were injected retro-orbitally with freshly isolated WT, KO or mixed (1:1 ratio) bone marrow cells (5×10^6 cells per mouse). All chimeras were provided antibiotic-containing water (40 mg trimethoprim and 200 mg sulfamethoxazole per 500 ml drinking water) for four weeks after irradiation and subsequently provided acidified water without antibiotics for a total of at least 8–12 weeks of reconstitution. The reconstitution of hematopoietic cells (proportion of donor $CD45^+$ cells among total $CD45^+$ cells) in the lung was analyzed by flow cytometry.

Infection of mice and lung harvest—Mice were anesthetized by intraperitoneal injection of ketamine (100 mg/kg) and xylazine (10 mg/kg) solution and then infected intranasally with *Legionella pneumophila* JR32 Δ*flaA* strain (10^6 CFU per mouse). At the indicated time points, the bronchoalveolar lavage (BAL) fluid was harvested with 1 ml cold PBS. The lung lobes were excised and digested with dissociation solution (20 U/ml DNase I, 240 U/ml Collagenase IV, and 5% FBS in PBS) at 37°C for 30 min. Mechanical dissociation of the lung tissue was performed using the Miltenyi GentleMACS™ Dissociator. The lung homogenates were incubated with red blood cell lysis buffer on ice for 5 min and then quenched with cold PBS. The cell pellet was resuspended with FACS buffer to generate a single cell suspension and then filtered through nylon mesh prior to flow cytometric analysis. To measure bacterial CFUs within the lung, lung lobes were excised and placed into in 5 ml sterile water, homogenized using the Miltenyi GentleMACS™ Dissociator, and cell lysates were then plated onto CYE agar plates. Bacterial loads were determined by calculating the number of bacterial colony forming units (CFU) per gram of lung (CFU/g).

Administration of tamoxifen—Tamoxifen (TXF) was a 40 mg/ml stock solution in corn oil. Four consecutive doses of TXF (0.2 mg/g body weight as a single daily dose) were intraperitoneally (IP) injected into *Il1r1*$^{fl/fl}$;*Spc-creER*^{T2} or *Il1r1*$^{r/r}$;*Spc-creER*^{T2} mice and

its littermate controls at 8 weeks of age to induce recombination. *Il1r1* deletion or restore efficiency in these mice were analyzed at least 4 days after the final injection of TXF.

Neutralization of GM-CSF *in vivo*—C57BL/6J mice were IP injected with 250 μg of anti-GM-CSF antibodies or 250 μg of isotype control antibodies 16 hours prior to infection, followed by a second injection when mice were infected. For experiments in which bacterial loads in the lungs at 72 hpi were measured, mice were also IP injected at days 1 and 2 post-infection with 125 μg of anti-GM-CSF or isotype antibodies.

Cytokine production assays—For in vivo experiments, the first 1 ml of BAL was used for cytokine measurements. For in vitro experiments, tissue culture plates containing cells were centrifuged 5 min at 300 g, and then supernatants were collected for analysis. Most cytokines were measured using commercial mouse ELISA kits (see Key Resources Table). IL-12 was measured by ELISA using purified anti-mouse IL-12 p40/70 antibody and biotin rat anti-mouse IL-12 p40/70 antibody. The Luminex assay was performed using the MILLIPLEX™ Mouse Cytokine/Chemokine Magnetic Bead Panel with technical assistance from the Human Immunology Core at the University of Pennsylvania Perelman School of Medicine.

Flow cytometry—To analyze cell populations in the BAL and lung, cell suspensions were treated with fluorescent Zombie Yellow™ dye (live/dead stain) for 15 min at RT. Anti-CD16/CD32 antibody was used to block Fc receptors. Fluorescently conjugated antibodies, including anti-CD45, anti-CD45.1, anti-CD45.2, antiLy6G, anti-Ly6C, anti-Siglec F, anti-CD11c, anti-CD11b, anti-MHC II, anti-CD31, anti-EpCAM, anti-T1a, anti-Sca-1, and anti-CD49f, were used for surface staining. To distinguish MCs distally within the systemic circulation (peripheral blood MCs) or locally within the lung, including those within or adhered to the pulmonary vasculature (vascular MCs) and those that entered the lung interstitium (interstitial MCs), *L.p.*-infected or naïve WT mice were intravenously (IV) injected with PE-labeled anti-CD45 antibodies three minutes prior to harvesting of lung tissue to label all circulating MCs, followed by staining of all lung cells with anti-CD45-Alexa Fluor (AF) 488 antibodies. For intracellular cytokine staining, cell suspensions were incubated with Brefeldin A (0.1%) and monensin (0.066%) solution for 4 hours at 37°C prior to all staining, treated with BD Cytofix/Cytoperm™ buffer for 20 min at 4°C, and stained with antibodies specific for TNFα, IL-12, IL-1α, or IL-1β in perm/wash buffer for 30 min at 4°C, or stained with biotinylated anti-GM-CSF antibody, followed by incubation with APC-labeled streptavidin. Isotype antibodies were used as negative controls. For reactive oxygen species (ROS) measurements, cell suspensions were incubated with CellROX™ Deep Red reagent at a final concentration of 5 μM at for 30 min at 37°C, then immediately analyzed on the BD LSR II flow cytometer. Data were analyzed with FlowJo software v10.3.

Fluorescence-activated cell sorting of lung cell subsets—Single cell lung suspensions were incubated with Zombie Yellow™ dye, anti-CD16/CD32 antibody, and fluorescently-labeled antibodies (see Key Resources Table). Non-hematopoietic cell subsets were identified as follows: alveolar type II epithelial cell

(AECII, $CD45^{-}CD31^{-}EpCAM^{+}CD49f^{low}T1a^{-}$), alveolar type I epithelial cell (AECI, $CD45^{-}CD31^{-}EpCAM^{+}CD49f^{low}T1a^{+}$), endothelial cell (EnC, $CD45CD31^{+}EpCAM^{-}$), bronchial alveolar stem cell (BASC, $CD45^{-}CD31^{-}EpCAM^{hi}CD49f^{hi}Sca\text{-}1^{+}$). Hematopoietic cell subsets were identified as follows: neutrophil (NΦ, $CD45^{+}Ly6G^{+}CD11b^{+}$), alveolar macrophage (AMΦ, $CD45^{+}SiglecF^{+}CD11c^{+}CD11b^{-}$), monocyte (MC, $CD45^{+}Ly6G^{-}SiglecF^{-}CD11cCD11b^{+}Ly6C^{high}$), conventional dendritic cell (cDC, $CD45^{+}Ly6G^{-}SiglecF^{-}MHCII^{hi}CD11c^{hi}$), NK cell ($CD45^{+}CD3^{-}NK1.1^{+}$), NKT cell ($CD45^{+}CD3^{+}NK1.1^{+}$), αβT cell ($CD45^{+}CD3^{+}TCR\beta^{+}$), and γδT cell ($CD45^{+}CD3^{+}TCR\gamma/\delta^{+}$). Individual cell types were isolated using a BD FACSAria™ Cell Sorter.

RNA isolation and quantitative RT-PCR—Total RNA was isolated using RNeasy Mini Kit. cDNA was generated using SuperScript II Reverse Transcriptase. Primers (see Supplemental Table S1) were synthesized by Integrated DNA Technologies, Inc. (Coralville, IA). Quantitative RT-PCR was performed using SsoFast™ EvaGreen® Supermix with Low ROX on a CFX96™ Real-Time PCR Detection System (Bio-Rad). RT-PCR amplification efficiency and specificity for each primer pair were determined by performing analysis of standard curves and melt curves. mRNA expression of each gene relative to *Gapdh* or *Hprt* was calculated using the formula $2^{-\Delta Ct}$.

Immunoblot analysis—Cells were lysed in 1x SDS-PAGE loading buffer supplemented with 1x Halt™ Protease and Phosphatase Inhibitor Cocktail. Protein samples were separated by SDS-PAGE and then transferred to PVDF membranes. Primary antibodies specific for pro-IL-1β (1:1000), GLUT1 (1:1000), HK2 (1:1000), PFKP (1:1000) and β-actin (1:1000) were used. Anti-rabbit or mouse HRP-linked IgG antibody was used as a secondary antibody (1:2000). Detection was performed using SuperSignal™ Substrates.

Glycolysis and oxidative phosphorylation analysis—Primary mouse bone marrow monocytes were obtained as described above and seeded into Seahorse XF96 cell culture microplates (10^5 cells per well) containing RPMI media with 10% FBS. Four hours later, the cells were infected with or without Lp02 Δ*flaA* strain (MOI=5), or stimulated with LPS (from *E. coli*, 10 ng/ml), followed by treatment with rGM-CSF or PBS. After 12 hours of stimulation, the media was replaced with fresh Seahorse XF base media supplemented with 2 mM L-glutamine for the glycolysis test, or additionally supplemented with 10 mM glucose and 1 mM pyruvate for the oxidative phosphorylation test, and pH was adjusted to 7.4. Plates were incubated without CO_2 for 45 min in a 37°C incubator and then loaded into the Seahorse XFe96 analyzer. The Seahorse XF Glycolysis Stress Test Kit and Cell Mito Stress Test Kit were used to measure the extracellular acidification rate (ECAR, mpH/min) and oxygen consumption rate (OCR, pmol/min), respectively. Glucose (10 mM), Oligomycin (1 μM) and 2-DG (50 mM) for ECAR measurements, and Oligomycin (1 μM), FCCP (1 μM) and Rot/AA (0.5 μM) for OCR measurements were injected at the indicated time points. ECAR and OCR were calculated using Wave software v2.4.

QUANTIFICATION AND STATISTICAL ANALYSIS

All statistical analyses were performed using GraphPad Prism software v7.0 and v8.0. Data are shown as bar graph or dot plots (mean ± SD) or violin plots (median). Statistical

significance was determined by performing t tests for two unpaired groups, Wilcoxon matched-pairs signed rank test for paired two groups, one-way ANOVA with Tukey's multiple comparisons test for three or more groups, or two-way ANOVA with Sidak's multiple comparisons test for experiments that have two factors with multiple comparisons as indicated in each figure legend. *P* values less than 0.05 were considered to be statistically significant. Information on number of biological and technical replicates can be found in the figure legends when appropriate.

Supplementary Material

Refer to Web version on PubMed Central for supplementary material.

Acknowledgements

We thank Igor Brodsky and Christopher Hunter for scientific advice, discussion, and critical reading of the manuscript; members of the Brodsky and Shin labs and Terri Laufer for insightful discussions and scientific advice; the Pancreatic Islet Cell Biology Core of the Institute for Diabetes, Obesity, and Metabolism for assistance with Seahorse assays; the Flow Cytometry and Cell Sorting Resource Laboratory for flow cytometric technical support; and Yoichiro Iwakura for generously providing *Il1a*$^{-/-}$ and *Il1b*$^{-/-}$ mice. This work was supported by NIH/NIAID grants R01AI118861 (SS) and R01AI123243 (SS), a Linda Pechenik Montague Investigator Award from the University of Pennsylvania Perelman School of Medicine (SS), and a Burroughs-Wellcome Fund Investigators in the Pathogenesis of Infectious Diseases Award (SS).

References

Anzai A, Choi JL, He S, Fenn AM, Nairz M, Rattik S, McAlpine CS, Mindur JE, Chan CT, Iwamoto Y, et al. (2017). The infarcted myocardium solicits GM-CSF for the detrimental oversupply of inflammatory leukocytes. J Exp Med 214, 3293–3310. [PubMed: 28978634]

Asrat S, Dugan AS, and Isberg RR (2014). The frustrated host response to Legionella pneumophila is bypassed by MyD88-dependent translation of pro-inflammatory cytokines. PLoS Pathog 10, e1004229.

Barry KC, Fontana MF, Portman JL, Dugan AS, and Vance RE (2013). IL-1alpha signaling initiates the inflammatory response to virulent Legionella pneumophila in vivo. J Immunol 190, 6329–6339. [PubMed: 23686480]

Barry KC, Ingolia NT, and Vance RE (2017). Global analysis of gene expression reveals mRNA superinduction is required for the inducible immune response to a bacterial pathogen. Elife 6.

Becher B, Tugues S, and Greter M (2016). GM-CSF: From Growth Factor to Central Mediator of Tissue Inflammation. Immunity 45, 963–973. [PubMed: 27851925]

Belyi Y, Tabakova I, Stahl M, and Aktories K (2008). Lgt: a family of cytotoxic glucosyltransferases produced by Legionella pneumophila. J Bacteriol 190, 3026–3035. [PubMed: 18281405]

Berger KH, and Isberg RR (1993). Two distinct defects in intracellular growth complemented by a single genetic locus in Legionella pneumophila. Mol Microbiol 7, 7–19. [PubMed: 8382332]

Bhattacharya J, and Westphalen K (2016). Macrophage-epithelial interactions in pulmonary alveoli. Semin Immunopathol 38, 461–469. [PubMed: 27170185]

Blau H, Riklis S, Kravtsov V, and Kalina M (1994). Secretion of cytokines by rat alveolar epithelial cells: possible regulatory role for SP-A. Am J Physiol 266, L148–155. [PubMed: 8141310]

Bogunovic M, Ginhoux F, Helft J, Shang L, Hashimoto D, Greter M, Liu K, Jakubzick C, Ingersoll MA, Leboeuf M, et al. (2009). Origin of the lamina propria dendritic cell network. Immunity 31, 513–525. [PubMed: 19733489]

Brieland JK, Remick DG, LeGendre ML, Engleberg NC, and Fantone JC (1998). In vivo regulation of replicative Legionella pneumophila lung infection by endogenous interleukin-12. Infect Immun 66, 65–69. [PubMed: 9423840]

Brown AS, Yang C, Fung KY, Bachem A, Bourges D, Bedoui S, Hartland EL, and van Driel IR (2016). Cooperation between Monocyte-Derived Cells and Lymphoid Cells in the Acute Response to a Bacterial Lung Pathogen. PLoS Pathog 12, e1005691.

Bustamente E, Morris HP, and Pedersen PL (1977). Hexokinase: the direct link between mitochondrial and glycolytic reactions in rapidly growing cancer cells. Adv Exp Med Biol 92, 363–380. [PubMed: 205103]

Case CL, Kohler LJ, Lima JB, Strowig T, de Zoete MR, Flavell RA, Zamboni DS, and Roy CR (2013). Caspase-11 stimulates rapid flagellin-independent pyroptosis in response to Legionella pneumophila. Proc Natl Acad Sci U S A 110, 1851–1856. [PubMed: 23307811]

Casson CN, Copenhaver AM, Zwack EE, Nguyen HT, Strowig T, Javdan B, Bradley WP, Fung TC, Flavell RA, Brodsky IE, et al. (2013). Caspase-11 activation in response to bacterial secretion systems that access the host cytosol. PLoS Pathog 9, e1003400.

Casson CN, Doerner JL, Copenhaver AM, Ramirez J, Holmgren AM, Boyer MA, Siddarthan IJ, Rouhanifard SH, Raj A, and Shin S (2017). Neutrophils and Ly6Chi monocytes collaborate in generating an optimal cytokine response that protects against pulmonary Legionella pneumophila infection. PLoS Pathog 13, e1006309.

Chang CH, Curtis JD, Maggi LB Jr., Faubert B, Villarino AV, O'Sullivan D, Huang SC, van der Windt GJ, Blagih J, Qiu J, et al. (2013). Posttranscriptional control of T cell effector function by aerobic glycolysis. Cell 153, 1239–1251. [PubMed: 23746840]

Chaplin DD (2010). Overview of the immune response. J Allergy Clin Immunol 125, S3–23. [PubMed: 20176265]

Copenhaver AM, Casson CN, Nguyen HT, Duda MM, and Shin S (2015). IL-1R signaling enables bystander cells to overcome bacterial blockade of host protein synthesis. Proc Natl Acad Sci U S A 112, 7557–7562. [PubMed: 26034289]

Copenhaver AM, Casson CN, Nguyen HT, Fung TC, Duda MM, Roy CR, and Shin S (2014). Alveolar macrophages and neutrophils are the primary reservoirs for Legionella pneumophila and mediate cytosolic surveillance of type IV secretion. Infect Immun 82, 4325–4336. [PubMed: 25092908]

Cousins DJ, Staynov DZ, and Lee TH (1994). Regulation of interleukin-5 and granulocyte-macrophage colony-stimulating factor expression. Am J Respir Crit Care Med 150, S50–53. [PubMed: 7952592]

Crapo JD, Barry BE, Gehr P, Bachofen M, and Weibel ER (1982). Cell number and cell characteristics of the normal human lung. Am Rev Respir Dis 126, 332–337. [PubMed: 7103258]

Croxford AL, Lanzinger M, Hartmann FJ, Schreiner B, Mair F, Pelczar P, Clausen BE, Jung S, Greter M, and Becher B (2015). The Cytokine GM-CSF Drives the Inflammatory Signature of CCR2+ Monocytes and Licenses Autoimmunity. Immunity 43, 502–514. [PubMed: 26341401]

Cunningham ET Jr., Wada E, Carter DB, Tracey DE, Battey JF, and De Souza EB (1992). In situ histochemical localization of type I interleukin-1 receptor messenger RNA in the central nervous system, pituitary, and adrenal gland of the mouse. J Neurosci 12, 1101–1114. [PubMed: 1532025]

De Leon JA, Qiu J, Nicolai CJ, Counihan JL, Barry KC, Xu L, Lawrence RE, Castellano BM, Zoncu R, Nomura DK, et al. (2017). Positive and Negative Regulation of the Master Metabolic Regulator mTORC1 by Two Families of Legionella pneumophila Effectors. Cell Rep 21, 2031–2038. [PubMed: 29166595]

Dinarello CA (1998). Interleukin-1, interleukin-1 receptors and interleukin-1 receptor antagonist. Int Rev Immunol 16, 457–499. [PubMed: 9646173]

Dranoff G, Crawford AD, Sadelain M, Ream B, Rashid A, Bronson RT, Dickersin GR, Bachurski CJ, Mark EL, Whitsett JA, et al. (1994). Involvement of granulocyte-macrophage colony-stimulating factor in pulmonary homeostasis. Science 264, 713–716. [PubMed: 8171324]

Egea L, McAllister CS, Lakhdari O, Minev I, Shenouda S, and Kagnoff MF (2013). GM-CSF produced by nonhematopoietic cells is required for early epithelial cell proliferation and repair of injured colonic mucosa. J Immunol 190, 1702–1713. [PubMed: 23325885]

Everts B, Amiel E, Huang SC, Smith AM, Chang CH, Lam WY, Redmann V, Freitas TC, Blagih J, van der Windt GJ, et al. (2014). TLR-driven early glycolytic reprogramming via the kinases TBK1-IKKvarepsilon supports the anabolic demands of dendritic cell activation. Nat Immunol 15, 323–332. [PubMed: 24562310]

Fontana MF, Banga S, Barry KC, Shen X, Tan Y, Luo ZQ, and Vance RE (2011). Secreted bacterial effectors that inhibit host protein synthesis are critical for induction of the innate immune response to virulent Legionella pneumophila. PLoS Pathog 7, e1001289.

Fraser DW, Tsai TR, Orenstein W, Parkin WE, Beecham HJ, Sharrar RG, Harris J, Mallison GF, Martin SM, McDade JE, et al. (1977). Legionnaires' disease: description of an epidemic of pneumonia. N Engl J Med 297, 1189–1197. [PubMed: 335244]

Glaccum MB, Stocking KL, Charrier K, Smith JL, Willis CR, Maliszewski C, Livingston DJ, Peschon JJ, and Morrissey PJ (1997). Phenotypic and functional characterization of mice that lack the type I receptor for IL-1. J Immunol 159, 3364–3371. [PubMed: 9317135]

Greter M, Helft J, Chow A, Hashimoto D, Mortha A, Agudo-Cantero J, Bogunovic M, Gautier EL, Miller J, Leboeuf M, et al. (2012). GM-CSF controls nonlymphoid tissue dendritic cell homeostasis but is dispensable for the differentiation of inflammatory dendritic cells. Immunity 36, 1031–1046. [PubMed: 22749353]

Guilliams M, De Kleer I, Henri S, Post S, Vanhoutte L, De Prijck S, Deswarte K, Malissen B, Hammad H, and Lambrecht BN (2013). Alveolar macrophages develop from fetal monocytes that differentiate into long-lived cells in the first week of life via GM-CSF. J Exp Med 210, 1977–1992. [PubMed: 24043763]

Heath L, Chrisp C, Huffnagle G, LeGendre M, Osawa Y, Hurley M, Engleberg C, Fantone J, and Brieland J (1996). Effector mechanisms responsible for gamma interferon-mediated host resistance to Legionella pneumophila lung infection: the role of endogenous nitric oxide differs in susceptible and resistant murine hosts. Infect Immun 64, 5151–5160. [PubMed: 8945559]

Hernandez-Santos N, Wiesner DL, Fites JS, McDermott AJ, Warner T, Wuthrich M, and Klein BS (2018). Lung Epithelial Cells Coordinate Innate Lymphocytes and Immunity against Pulmonary Fungal Infection. Cell Host Microbe 23, 511–522 e515. [PubMed: 29576482]

Horai R, Asano M, Sudo K, Kanuka H, Suzuki M, Nishihara M, Takahashi M, and Iwakura Y (1998). Production of mice deficient in genes for interleukin (IL)-1alpha, IL-1beta, IL-1alpha/beta, and IL-1 receptor antagonist shows that IL-1beta is crucial in turpentine-induced fever development and glucocorticoid secretion. J Exp Med 187, 1463–1475. [PubMed: 9565638]

Huang FF, Barnes PF, Feng Y, Donis R, Chroneos ZC, Idell S, Allen T, Perez DR, Whitsett JA, Dunussi-Joannopoulos K, et al. (2011). GM-CSF in the lung protects against lethal influenza infection. Am J Respir Crit Care Med 184, 259–268. [PubMed: 21474645]

Huffman JA, Hull WM, Dranoff G, Mulligan RC, and Whitsett JA (1996). Pulmonary epithelial cell expression of GM-CSF corrects the alveolar proteinosis in GM-CSF-deficient mice. J Clin Invest 97, 649–655. [PubMed: 8609219]

Inaba K, Inaba M, Romani N, Aya H, Deguchi M, Ikehara S, Muramatsu S, and Steinman RM (1992). Generation of large numbers of dendritic cells from mouse bone marrow cultures supplemented with granulocyte/macrophage colony-stimulating factor. J Exp Med 176, 1693–1702. [PubMed: 1460426]

Isberg RR, O'Connor TJ, and Heidtman M (2009). The Legionella pneumophila replication vacuole: making a cosy niche inside host cells. Nat Rev Microbiol 7, 13–24. [PubMed: 19011659]

Iwasaki A, and Medzhitov R (2015). Control of adaptive immunity by the innate immune system. Nat Immunol 16, 343–353. [PubMed: 25789684]

Jung HC, Eckmann L, Yang SK, Panja A, Fierer J, Morzycka-Wroblewska E, and Kagnoff MF (1995). A distinct array of proinflammatory cytokines is expressed in human colon epithelial cells in response to bacterial invasion. J Clin Invest 95, 55–65. [PubMed: 7814646]

Kasahara S, Jhingran A, Dhingra S, Salem A, Cramer RA, and Hohl TM (2016). Role of Granulocyte-Macrophage Colony-Stimulating Factor Signaling in Regulating Neutrophil Antifungal Activity and the Oxidative Burst During Respiratory Fungal Challenge. J Infect Dis 213, 1289–1298. [PubMed: 26908736]

Kawai T, and Akira S (2007). Signaling to NF-kappaB by Toll-like receptors. Trends Mol Med 13, 460–469. [PubMed: 18029230]

Krawczyk CM, Holowka T, Sun J, Blagih J, Amiel E, DeBerardinis RJ, Cross JR, Jung E, Thompson CB, Jones RG, et al. (2010). Toll-like receptor-induced changes in glycolytic metabolism regulate dendritic cell activation. Blood 115, 4742–4749. [PubMed: 20351312]

Langston PK, Shibata M, and Horng T (2017). Metabolism Supports Macrophage Activation. Front Immunol 8, 61. [PubMed: 28197151]

LeibundGut-Landmann S, Weidner K, Hilbi H, and Oxenius A (2011). Nonhematopoietic cells are key players in innate control of bacterial airway infection. J Immunol 186, 3130–3137. [PubMed: 21270399]

Liu X, and Shin S (2019). Viewing Legionella pneumophila pathogenesis through an immunological lens. J Mol Biol.

Liu X, Yamashita T, Chen Q, Belevych N, McKim DB, Tarr AJ, Coppola V, Nath N, Nemeth DP, Syed ZW, et al. (2015). Interleukin 1 type 1 receptor restore: a genetic mouse model for studying interleukin 1 receptor-mediated effects in specific cell types. J Neurosci 35, 2860–2870. [PubMed: 25698726]

McDade JE, Shepard CC, Fraser DW, Tsai TR, Redus MA, and Dowdle WR (1977). Legionnaires' disease: isolation of a bacterium and demonstration of its role in other respiratory disease. N Engl J Med 297, 1197–1203. [PubMed: 335245]

Mills EL, Kelly B, Logan A, Costa ASH, Varma M, Bryant CE, Tourlomousis P, Dabritz JHM, Gottlieb E, Latorre I, et al. (2016). Succinate Dehydrogenase Supports Metabolic Repurposing of Mitochondria to Drive Inflammatory Macrophages. Cell 167, 457–470 e413. [PubMed: 27667687]

Molofsky AB, Byrne BG, Whitfield NN, Madigan CA, Fuse ET, Tateda K, and Swanson MS (2006). Cytosolic recognition of flagellin by mouse macrophages restricts Legionella pneumophila infection. J Exp Med 203, 1093–1104. [PubMed: 16606669]

Mortha A, Chudnovskiy A, Hashimoto D, Bogunovic M, Spencer SP, Belkaid Y, and Merad M (2014). Microbiota-dependent crosstalk between macrophages and ILC3 promotes intestinal homeostasis. Science 343, 1249288.

Moss SM, Taylor IR, Ruggero D, Gestwicki JE, Shokat KM, and Mukherjee S (2019). A Legionella pneumophila Kinase Phosphorylates the Hsp70 Chaperone Family to Inhibit Eukaryotic Protein Synthesis. Cell Host Microbe 25, 454–462 e456. [PubMed: 30827827]

Mui AL, Wakao H, O'Farrell AM, Harada N, and Miyajima A (1995). Interleukin-3, granulocyte-macrophage colony stimulating factor and interleukin-5 transduce signals through two STAT5 homologs. EMBO J 14, 1166–1175. [PubMed: 7720707]

Na YR, Gu GJ, Jung D, Kim YW, Na J, Woo JS, Cho JY, Youn H, and Seok SH (2016). GM-CSF Induces Inflammatory Macrophages by Regulating Glycolysis and Lipid Metabolism. J Immunol 197, 4101–4109. [PubMed: 27742831]

Nagai H, and Kubori T (2011). Type IVB Secretion Systems of Legionella and Other Gram-Negative Bacteria. Front Microbiol 2, 136. [PubMed: 21743810]

Nimer SD, and Uchida H (1995). Regulation of granulocyte-macrophage colony-stimulating factor and interleukin 3 expression. Stem Cells 13, 324–335. [PubMed: 7549890]

Pang IK, Ichinohe T, and Iwasaki A (2013). IL-1R signaling in dendritic cells replaces pattern-recognition receptors in promoting CD8(+) T cell responses to influenza A virus. Nat Immunol 14, 246–253. [PubMed: 23314004]

Ponomarev ED, Shriver LP, Maresz K, Pedras-Vasconcelos J, Verthelyi D, and Dittel BN (2007). GM-CSF production by autoreactive T cells is required for the activation of microglial cells and the onset of experimental autoimmune encephalomyelitis. J Immunol 178, 39–48. [PubMed: 17182538]

Qiu J, and Luo ZQ (2017). Legionella and Coxiella effectors: strength in diversity and activity. Nat Rev Microbiol 15, 591–605. [PubMed: 28713154]

Quelle FW, Sato N, Witthuhn BA, Inhorn RC, Eder M, Miyajima A, Griffin JD, and Ihle JN (1994). JAK2 associates with the beta c chain of the receptor for granulocyte-macrophage colony-stimulating factor, and its activation requires the membrane-proximal region. Mol Cell Biol 14, 4335–4341. [PubMed: 8007942]

Ren T, Zamboni DS, Roy CR, Dietrich WF, and Vance RE (2006). Flagellin-deficient Legionella mutants evade caspase-1- and Naip5-mediated macrophage immunity. PLoS Pathog 2, e18. [PubMed: 16552444]

Robb L, Drinkwater CC, Metcalf D, Li R, Kontgen F, Nicola NA, and Begley CG (1995). Hematopoietic and lung abnormalities in mice with a null mutation of the common beta subunit of

the receptors for granulocyte-macrophage colony-stimulating factor and interleukins 3 and 5. Proc Natl Acad Sci U S A 92, 9565–9569. [PubMed: 7568173]

Robson MJ, Zhu CB, Quinlan MA, Botschner DA, Baganz NL, Lindler KM, Thome JG, Hewlett WA, and Blakely RD (2016). Generation and Characterization of Mice Expressing a Conditional Allele of the Interleukin-1 Receptor Type 1. PLoS One 11, e0150068.

Rock JR, Barkauskas CE, Cronce MJ, Xue Y, Harris JR, Liang J, Noble PW, and Hogan BL (2011). Multiple stromal populations contribute to pulmonary fibrosis without evidence for epithelial to mesenchymal transition. Proc Natl Acad Sci U S A 108, E1475–1483. [PubMed: 22123957]

Rodriguez-Prados JC, Traves PG, Cuenca J, Rico D, Aragones J, Martin-Sanz P, Cascante M, and Bosca L (2010). Substrate fate in activated macrophages: a comparison between innate, classic, and alternative activation. J Immunol 185, 605–614. [PubMed: 20498354]

Rothchild AC, Jayaraman P, Nunes-Alves C, and Behar SM (2014). iNKT cell production of GM-CSF controls Mycobacterium tuberculosis. PLoS Pathog 10, e1003805.

Roy CR, Berger KH, and Isberg RR (1998). Legionella pneumophila DotA protein is required for early phagosome trafficking decisions that occur within minutes of bacterial uptake. Mol Microbiol 28, 663–674. [PubMed: 9632267]

Sadosky AB, Wiater LA, and Shuman HA (1993). Identification of Legionella pneumophila genes required for growth within and killing of human macrophages. Infect Immun 61, 5361–5373. [PubMed: 8225610]

Schneider C, Nobs SP, Kurrer M, Rehrauer H, Thiele C, and Kopf M (2014). Induction of the nuclear receptor PPAR-gamma by the cytokine GM-CSF is critical for the differentiation of fetal monocytes into alveolar macrophages. Nat Immunol 15, 1026–1037. [PubMed: 25263125]

Shen X, Banga S, Liu Y, Xu L, Gao P, Shamovsky I, Nudler E, and Luo ZQ (2009). Targeting eEF1A by a Legionella pneumophila effector leads to inhibition of protein synthesis and induction of host stress response. Cell Microbiol 11, 911–926. [PubMed: 19386084]

Sherwood RK, and Roy CR (2016). Autophagy Evasion and Endoplasmic Reticulum Subversion: The Yin and Yang of Legionella Intracellular Infection. Annu Rev Microbiol 70, 413–433. [PubMed: 27607556]

Shibata Y, Berclaz PY, Chroneos ZC, Yoshida M, Whitsett JA, and Trapnell BC (2001). GM-CSF regulates alveolar macrophage differentiation and innate immunity in the lung through PU.1. Immunity 15, 557–567. [PubMed: 11672538]

Skerrett SJ, Bagby GJ, Schmidt RA, and Nelson S (1997). Antibody-mediated depletion of tumor necrosis factor-alpha impairs pulmonary host defenses to Legionella pneumophila. J Infect Dis 176, 1019–1028. [PubMed: 9333161]

Sonderegger I, Iezzi G, Maier R, Schmitz N, Kurrer M, and Kopf M (2008). GM-CSF mediates autoimmunity by enhancing IL-6-dependent Th17 cell development and survival. J Exp Med 205, 2281–2294. [PubMed: 18779348]

Stanley E, Lieschke GJ, Grail D, Metcalf D, Hodgson G, Gall JA, Maher DW, Cebon J, Sinickas V, and Dunn AR (1994). Granulocyte/macrophage colony-stimulating factor-deficient mice show no major perturbation of hematopoiesis but develop a characteristic pulmonary pathology. Proc Natl Acad Sci U S A 91, 5592–5596. [PubMed: 8202532]

Tannahill GM, Curtis AM, Adamik J, Palsson-McDermott EM, McGettrick AF, Goel G, Frezza C, Bernard NJ, Kelly B, Foley NH, et al. (2013). Succinate is an inflammatory signal that induces IL-1beta through HIF-1alpha. Nature 496, 238–242. [PubMed: 23535595]

Thorley AJ, Ford PA, Giembycz MA, Goldstraw P, Young A, and Tetley TD (2007). Differential regulation of cytokine release and leukocyte migration by lipopolysaccharide-stimulated primary human lung alveolar type II epithelial cells and macrophages. J Immunol 178, 463–473. [PubMed: 17182585]

Tugues S, Amorim A, Spath S, Martin-Blondel G, Schreiner B, De Feo D, Lutz M, Guscetti F, Apostolova P, Haftmann C, et al. (2018). Graft-versus-host disease, but not graft-versus-leukemia immunity, is mediated by GM-CSF-licensed myeloid cells. Sci Transl Med 10.

Ueda Y, Cain DW, Kuraoka M, Kondo M, and Kelsoe G (2009). IL-1R Type I-Dependent Hemopoietic Stem Cell Proliferation Is Necessary for Inflammatory Granulopoiesis and Reactive Neutrophilia. J Immunol 182, 6477–6484. [PubMed: 19414802]

Vogel JP, Andrews HL, Wong SK, and Isberg RR (1998). Conjugative transfer by the virulence system of Legionella pneumophila. Science 279, 873–876. [PubMed: 9452389]

Wang F, Zhang S, Vuckovic I, Jeon R, Lerman A, Folmes CD, Dzeja PP, and Herrmann J (2018). Glycolytic Stimulation Is Not a Requirement for M2 Macrophage Differentiation. Cell Metab 28, 463–475 e464. [PubMed: 30184486]

Weinberg F, Hamanaka R, Wheaton WW, Weinberg S, Joseph J, Lopez M, Kalyanaraman B, Mutlu GM, Budinger GR, and Chandel NS (2010). Mitochondrial metabolism and ROS generation are essential for Kras-mediated tumorigenicity. Proc Natl Acad Sci U S A 107, 8788–8793. [PubMed: 20421486]

Westphalen K, Gusarova GA, Islam MN, Subramanian M, Cohen TS, Prince AS, and Bhattacharya J (2014). Sessile alveolar macrophages communicate with alveolar epithelium to modulate immunity. Nature 506, 503–506. [PubMed: 24463523]

Wick AN, Drury DR, Nakada HI, and Wolfe JB (1957). Localization of the primary metabolic block produced by 2-deoxyglucose. J Biol Chem 224, 963–969. [PubMed: 13405925]

Willart MA, Deswarte K, Pouliot P, Braun H, Beyaert R, Lambrecht BN, and Hammad H (2012). Interleukin-1alpha controls allergic sensitization to inhaled house dust mite via the epithelial release of GM-CSF and IL-33. J Exp Med 209, 1505–1517. [PubMed: 22802353]

Zamboni DS, Kobayashi KS, Kohlsdorf T, Ogura Y, Long EM, Vance RE, Kuida K, Mariathasan S, Dixit VM, Flavell RA, et al. (2006). The Birc1e cytosolic pattern-recognition receptor contributes to the detection and control of Legionella pneumophila infection. Nat Immunol 7, 318–325. [PubMed: 16444259]

Highlights

- The alveolar epithelium serves as a central signal relay in antibacterial defense
- The alveolar epithelium produces GM-CSF in response to IL-1 during infection
- Cell-intrinsic GM-CSF signaling amplifies cytokine production by Ly6C^{hi} MCs
- Enhanced glycolysis mediates GM-CSF-dependent inflammatory gene expression

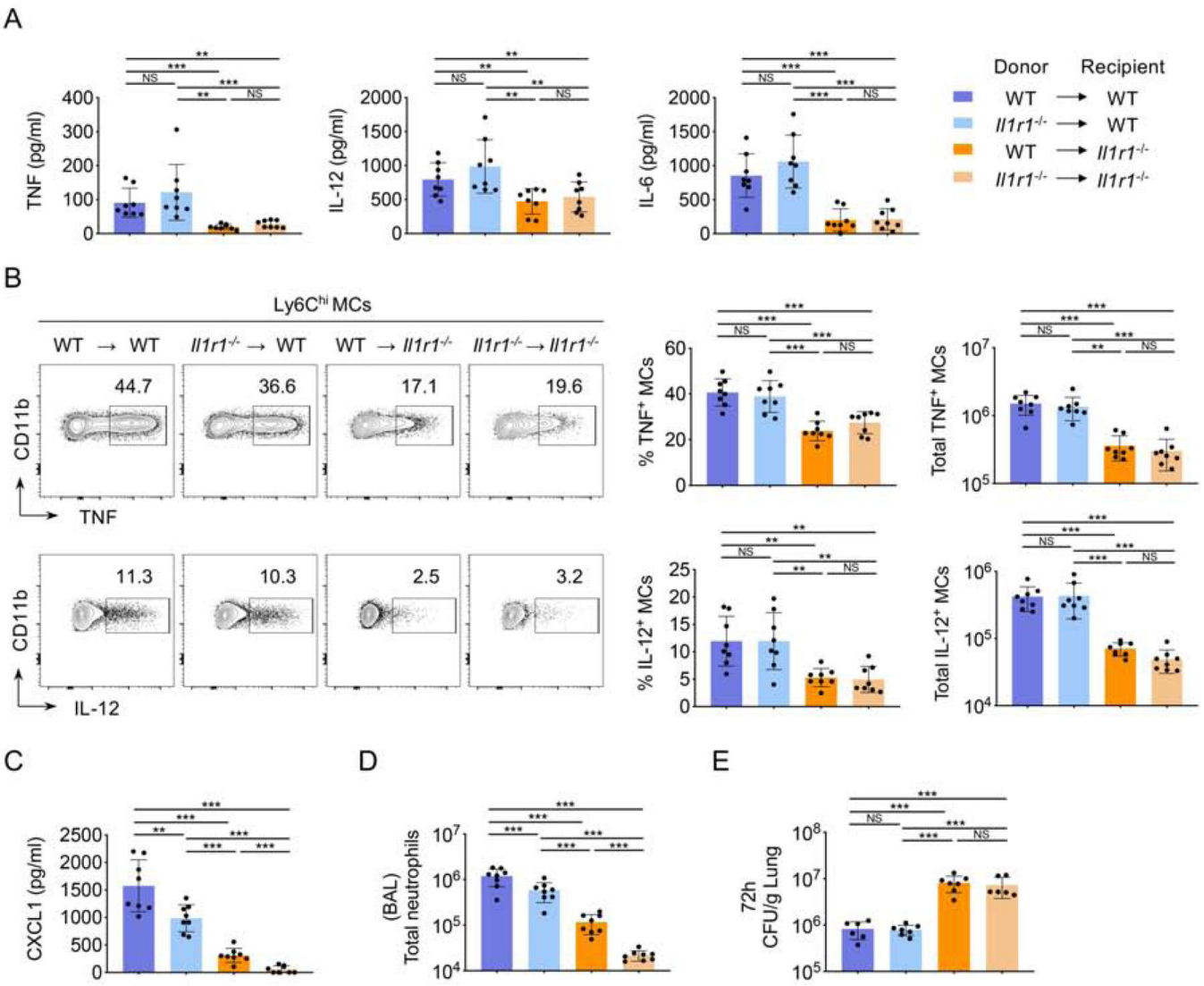

Figure 1. IL-1R signaling in nonhematopoietic cells orchestrates inflammation and antibacterial defense

(A) TNF, IL-6, and IL-12 levels in the bronchoalveolar lavage (BAL) of the indicated BM chimeras at 24 hours post-infection (hpi)

(B) Representative flow cytometric plots showing intracellular staining for TNF and IL-12 in Ly6C^{hi} MCs from the lungs at 24 hpi. Frequency and total number of TNF- and IL-12-producing MCs are shown.

(C and D) CXCL1 levels (C) and total number of neutrophils (D) in the BAL at 24 hpi.

(E) *Legionella* (*L.p.*) CFUs in the lungs of chimeras at 72 hpi.

Data shown are the pooled results of two independent experiments with 3–4 mice per group in each experiment. NS, not significant; **p < 0.01; and ***p < 0.001 (one-way ANOVA with Turkey's multiple comparisons test). Data are represented as mean ± SD.

See also Figure S1.

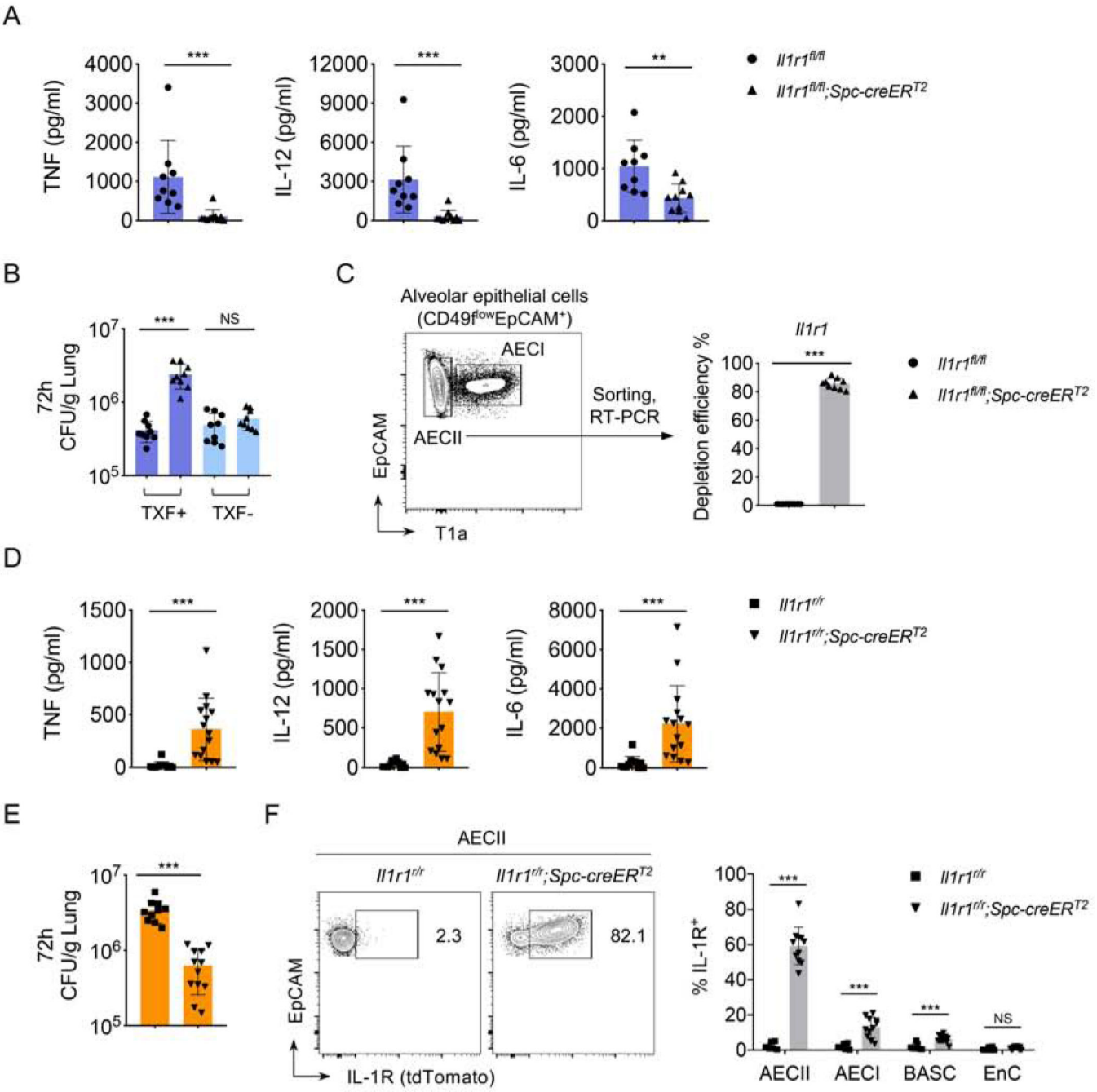

Figure 2. IL-1R expression on alveolar type II epithelial cells (AECII) is necessary and sufficient for inflammatory cytokine responses and bacterial clearance

(A and B) TNF, IL-12 and IL-6 levels in the BAL of tamoxifen (TXF)-injected *Il1r1*$^{fl/fl}$;*Spc-creER*^{T2} and *Il1r1*$^{fl/fl}$ mice at 24 hpi (A). *L.p.* CFUs in the lungs of mice ± TXF injection at 72 hpi (B).

(C) Representative flow cytometric plot showing the brief gating strategy for AECII (CD49f^{low} EpCAM^{+}T1a^{-}). Graph shows *Il1r1* deletion efficiency in AECII from *Il1r1*$^{fl/fl}$;*Spc-creER*^{T2} mice relative to *Il1r1*$^{fl/fl}$ mice following TXF injection.

(D and E) TNF, IL-12 and IL-6 levels in the BAL at 24 hpi (D) and *L.p.* CFUs in the lungs at 72 hpi (E) of TXF-injected *Il1r1*$^{r/r}$;*Spc-creER*^{T2} and *Il1r1*$^{r/r}$ mice.

(F) Representative flow cytometric plots showing tdTomato fluorescence as a tracer of *Il1r1* expression in AECII from TXF-injected *Il1r1*$^{r/r}$;*Spc-creER*^{T2} and *Il1r1*$^{r/r}$ mice at 24 hpi. Graph depicts frequency of IL-1R-expressing AECII, alveolar type I epithelial cells (AECI), bronchial alveolar stem cells (BASC), and lung endothelial cells (EnC). See a more detailed gating strategy in Figure S2B.

Data shown are the pooled results of three independent experiments with 3–4 mice per group in each experiment. Data are represented as mean ± SD. NS, not significant; **$p < 0.01$; and ***$p < 0.001$ (unpaired t test).

See also Figure S2.

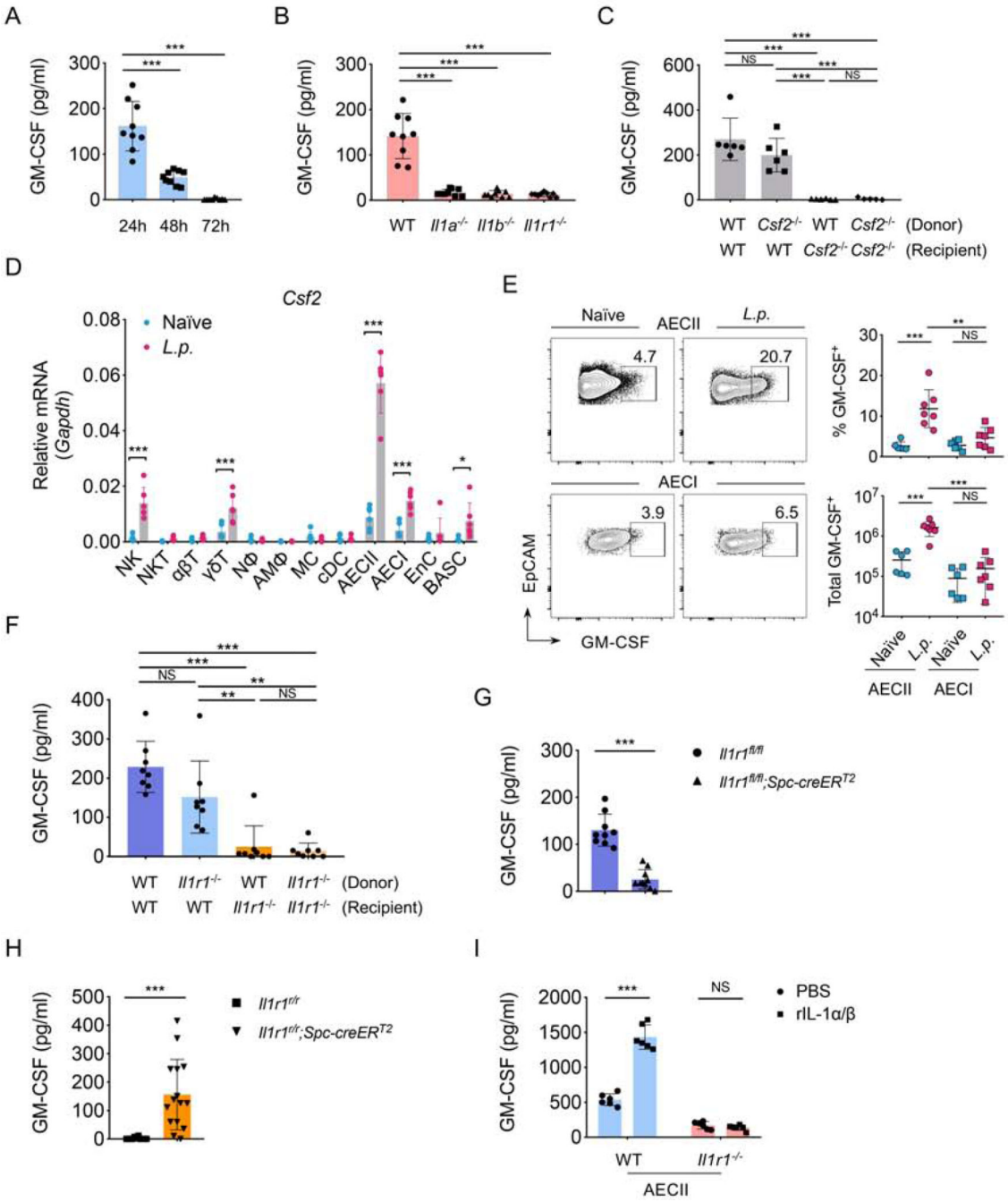

Figure 3. IL-1R signaling instructs AECII to produce GM-CSF during pulmonary *Legionella* infection

(A-C) GM-CSF levels in the BAL of C57BL/6J mice at 24, 48, and 72 hpi (A), WT, *Il1a*$^{-/-}$, *Il1b*$^{-/-}$ and *Il1r*$^{-/-}$ mice at 24 hpi (B), and WT:*Csf2* BM chimeras at 24 hpi (C).

(D) Csf2 transcript levels in the indicated cell types isolated from the lungs of naïve and *L.p.*-infected C57BL/6J mice at 24 hpi.

(E) Representative flow cytometric plots showing intracellular staining for GM-CSF in AECII and AECI from the lungs of naïve and *L.p.*-infected C57BL/6J mice at 24 hpi. Frequency and total number of GM-CSF-producing AECII and AECI.

(F-H) GM-CSF levels in the BAL of WT:*Il1r1*$^{-/-}$ BM chimeras (F), *Il1r1*$^{fl/fl}$;*Spc-creER*^{T2} and *Il1r1*$^{fl/fl}$ mice (G), and *Il1r1*$^{r/r}$;*Spc-creER*^{T2} and *Il1r1*$^{r/r}$ mice (H) at 24 hpi.
(I) GM-CSF levels in the supernatants of primary WT or *Il1r1*$^{-/-}$ AECII treated with 10 ng/ml each of recombinant IL-1α and IL-1β (rIL-1α/β) or PBS (vehicle control) and infected with *L.p.* (MOI=5) at 12 hpi.
Data shown are the pooled results of three (A, B, G, and H) or two (C-F) independent experiments with 3–4 mice per condition in each experiment. Data shown in I are the pooled results of two independent experiments with 3 mice and triplicate wells per condition in each experiment. Data are represented as mean ± SD. NS, not significant; *p<0.05; **p<0.01; and ***p<0.001 (one-way ANOVA with Turkey's multiple comparisons test for A-C and F; unpaired t test for D, E and G-I).
See also Figure S2.

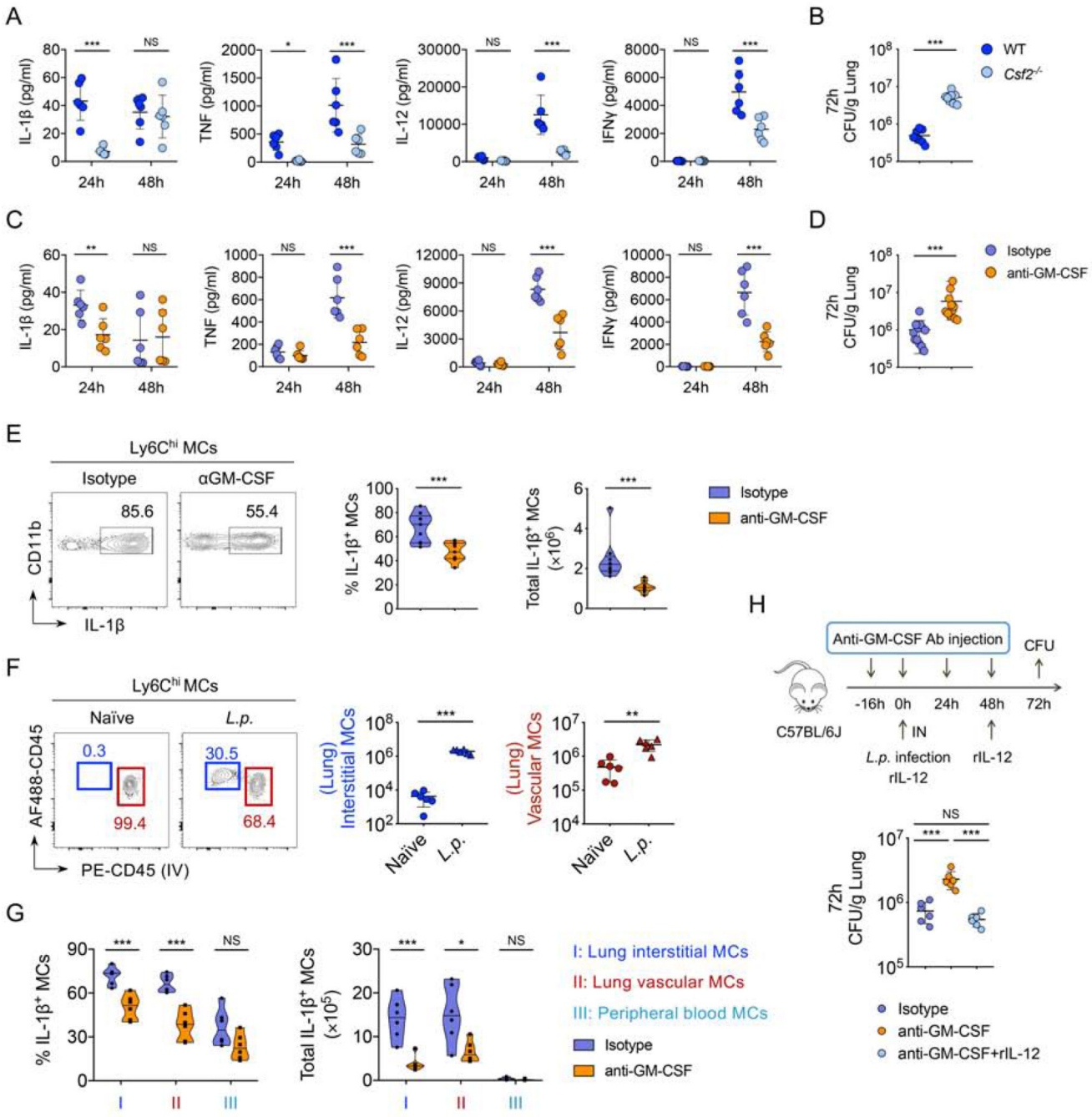

Figure 4. GM-CSF is required for local cytokine production by MCs within the lung and bacterial clearance

(A-D) IL-1β, TNF, IL-12, and IFNγ levels in the BAL at 24 and 48 hpi and *L.p.* CFUs in the lungs at 72 hpi of WT and *Csf2*$^{-/-}$ mice (A and B) or anti-GM-CSF and isotype control antibodies (Ab)-treated mice (C and D).

(E) Representative flow cytometric plots showing intracellular staining for IL-1β in Ly6C^{hi} MCs from the lungs of anti-GM-CSF or isotype Ab-treated mice infected with *L.p.* at 24 hpi. Frequency and total number of IL-1β-producing MCs are shown.

(F) Representative flow cytometric plots showing the percentages of interstitial MCs (AF488-CD45$^+$, PE-CD45$^-$) and vascular MCs (AF488-CD45$^+$, PE-CD45$^+$) in the lungs of *L.p.*-infected and naïve mice at 24 hpi. The total number of interstitial and vascular MCs in the lungs were quantified at 24 hpi.

(G) Percentage and total number of IL-1β-producing MCs from the interstitial or vascular lung compartments or the peripheral blood of infected mice administered anti-GM-CSF or isotype Ab at 24 hpi.

(H) *L.p.* CFUs in the lungs at 72 hpi of C57BL/6J mice intraperitoneally injected with anti-GM-CSF or isotype Ab (see Experimental Details) or a third group injected with anti-GM-CSF Ab provided 500 ng recombinant IL-12 p70 (rIL-12) intranasally (IN) at the time of infection and at day 2 post-infection.

Data shown are the pooled results of two (A-C and F-H) or three (D and E) independent experiments with 3–4 mice per condition for each experiment. Data are represented as mean ± SD for dot plots or median for violin plots. NS, not significant; *p<0.05; **p < 0.01; and ***p < 0.001 (unpaired t test for AG; one-way ANOVA with Turkey's multiple comparisons test for H).

See also Figure S3.

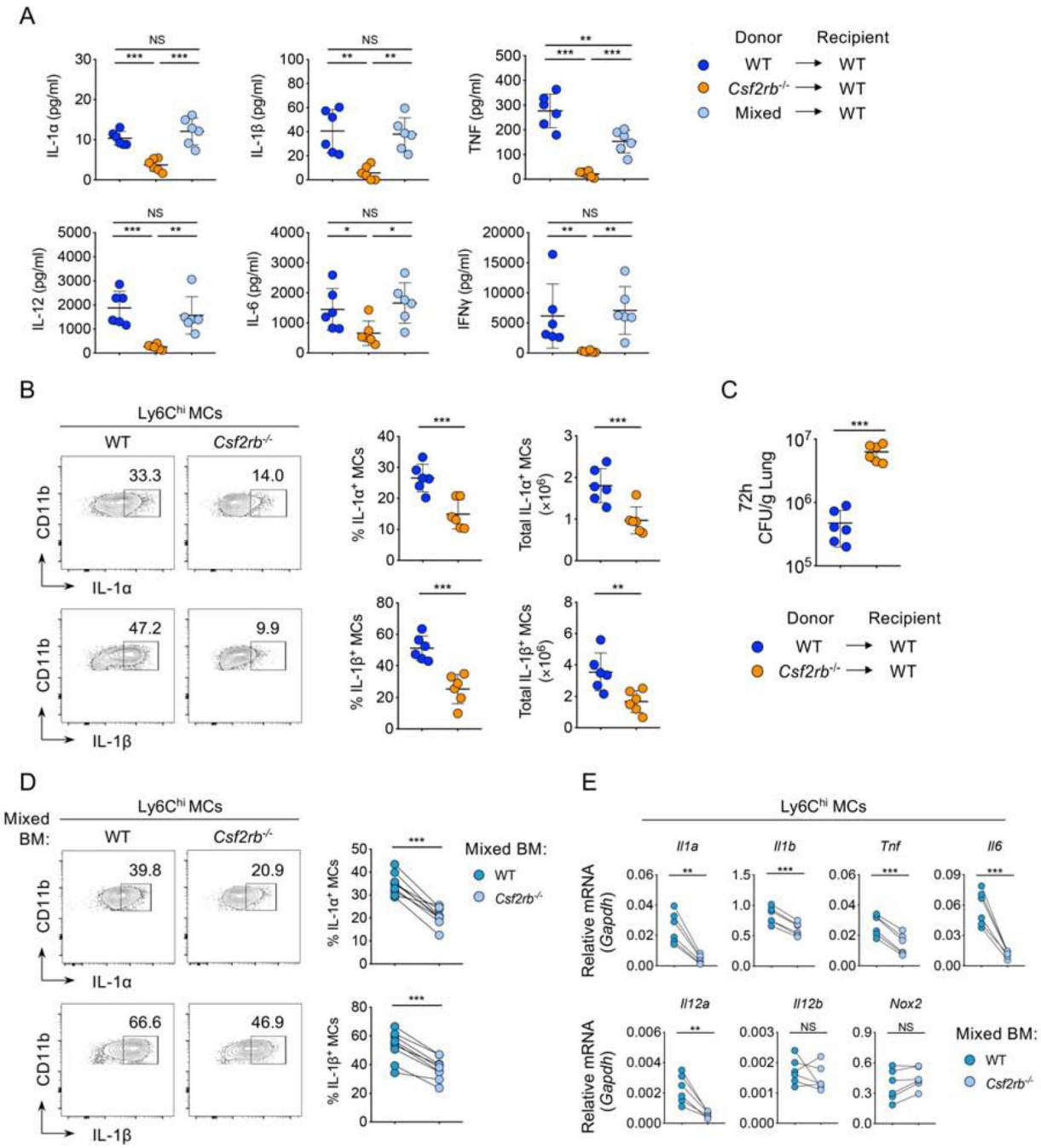

Figure 5. Monocyte-intrinsic GM-CSF receptor signaling is required for inflammatory cytokine production following infection

(A) IL-1α, IL-1β, TNF, IL-12 and IL-6 levels in the BAL at 24 hpi and IFNγ at 48 hpi of the BM chimeras.

(B) Representative flow cytometric plots showing intracellular staining for IL-1α and IL-1β in Ly6C^{hi} MCs from the lungs of chimeric WT→WT and *Csf2rb*$^{-/-}$→WT mice at 24 hpi. Graphs depict the frequency and total numbers of IL-1α- and IL-1β-producing Ly6C^{hi} MCs at 24 hpi.

(C) *L.p.* CFUs in the lungs of chimeric WT→WT and *Csf2rb*$^{-/-}$→WT mice at 72 hpi.

(D) Representative flow cytometric plots and graphs depicting the frequency of IL-1α^{+} or IL-1β^{+} WT or *Csf2rb*$^{-/-}$ MCs from the lungs of 50% WT/50% *Csf2rb*$^{-/-}$→WT mixed BM chimeras at 24 hpi. Each line represents the paired values of WT and *Csf2rb*$^{-/-}$ cells from a given mouse.

(E) *Il1a, Il1b, Tnf, Il6, Il12a, Il12b,* and *Nox2* transcript levels in Ly6C^{hi} MCs isolated from the lungs of 50% WT/50% *Csf2rb*$^{-/-}$→WT mixed BM chimeras at 24 hpi, as quantified by qRT-PCR. Each line represents the paired values of WT and *Csf2rb*$^{-/-}$ cells from a given mouse.

Data shown are the pooled results of two (A-C, and E) or three (D) independent experiments with 3 chimeric mice in each experiment. Data are represented as mean ± SD (A-C). NS, not significant; *p < 0.05; ***p < 0.01; and ***p < 0.001 (one-way ANOVA with Turkey's multiple comparisons test for A; unpaired t test for B and C; Wilcoxon matched-pairs signed rank test for D and E).

See also Figure S4.

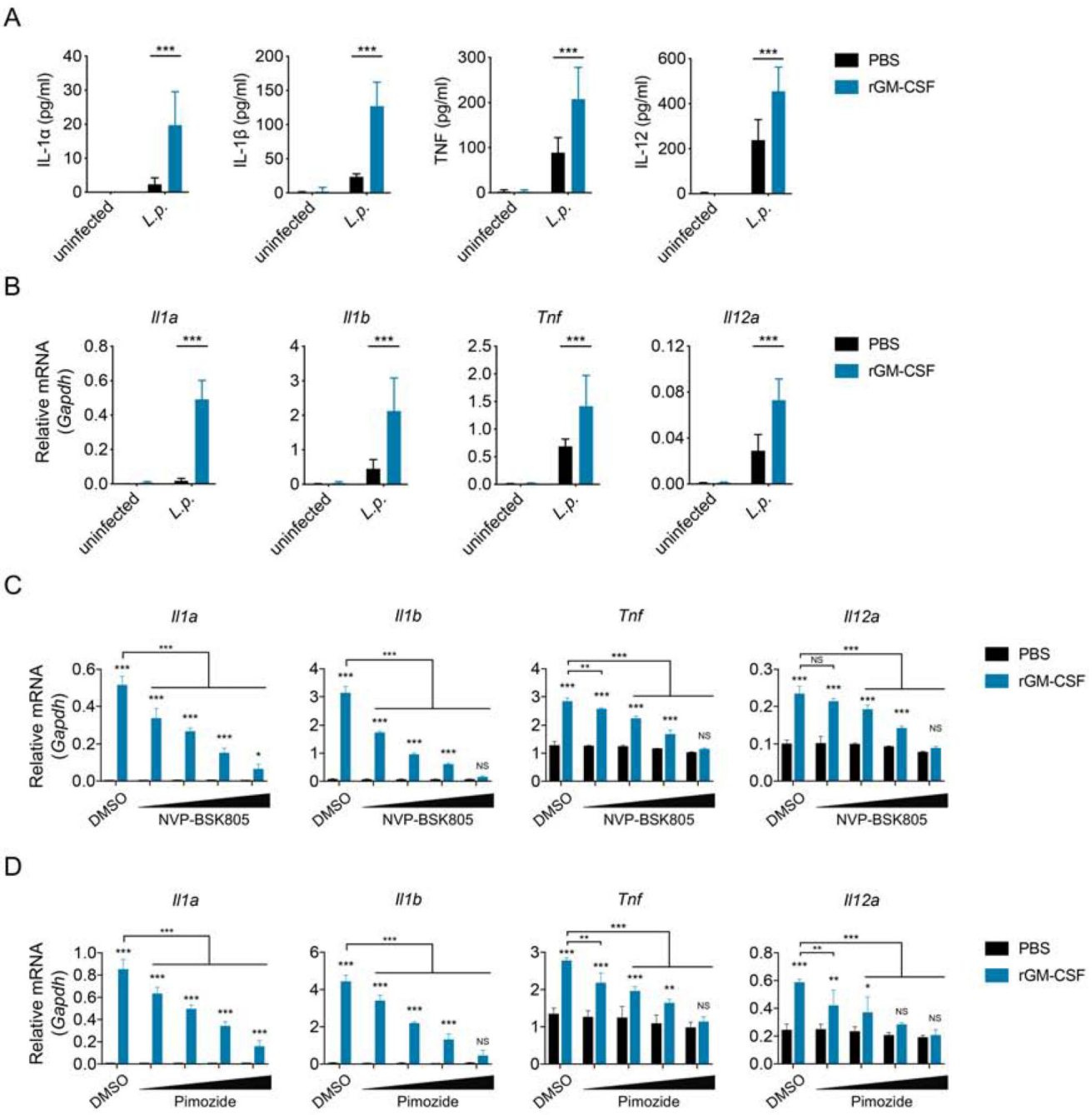

Figure 6. GM-CSF-dependent JAK2/STAT5 signaling is required for inflammatory cytokine expression

(A) Isolated WT MCs were uninfected or infected with *L.p.* (MOI=5) and given 10 ng/mL rGM-CSF or PBS. IL-1α, IL-1β, TNF, and IL-12 levels in the supernatants of MCs at 12 hpi are shown.

(B) *Il1a*, *Il1b*, *Tnf,* and *Il12a* transcript levels in *L.p.*-infected MCs supplemented with 10 ng/mL rGM-CSF or PBS at 12 hpi.

(C and D) *Il1a*, *Il1b*, *Tnf,* and *Il12a* transcript levels in MCs infected with *L.p.* (MOI=5), supplemented with 10 ng/mL rGM-CSF or PBS, and treated with JAK2 inhibitor NVP-

BSK805 (250, 500, 1000, or 2000 nM) (C), STAT5 inhibitor Pimozide (1, 2, 2.5, or 5 μM) (D), or DMSO vehicle control, at 12 hpi.

Data shown are the pooled results of three (A and B) or two (C and D) independent experiments. Data are represented as mean ± SD. NS, not significant; *$p < 0.05$; **$p < 0.01$; and ***$p < 0.001$ (unpaired t test for A and B; two-way ANOVA with Sidak's multiple comparisons test for C and D).

See also Figure S5.

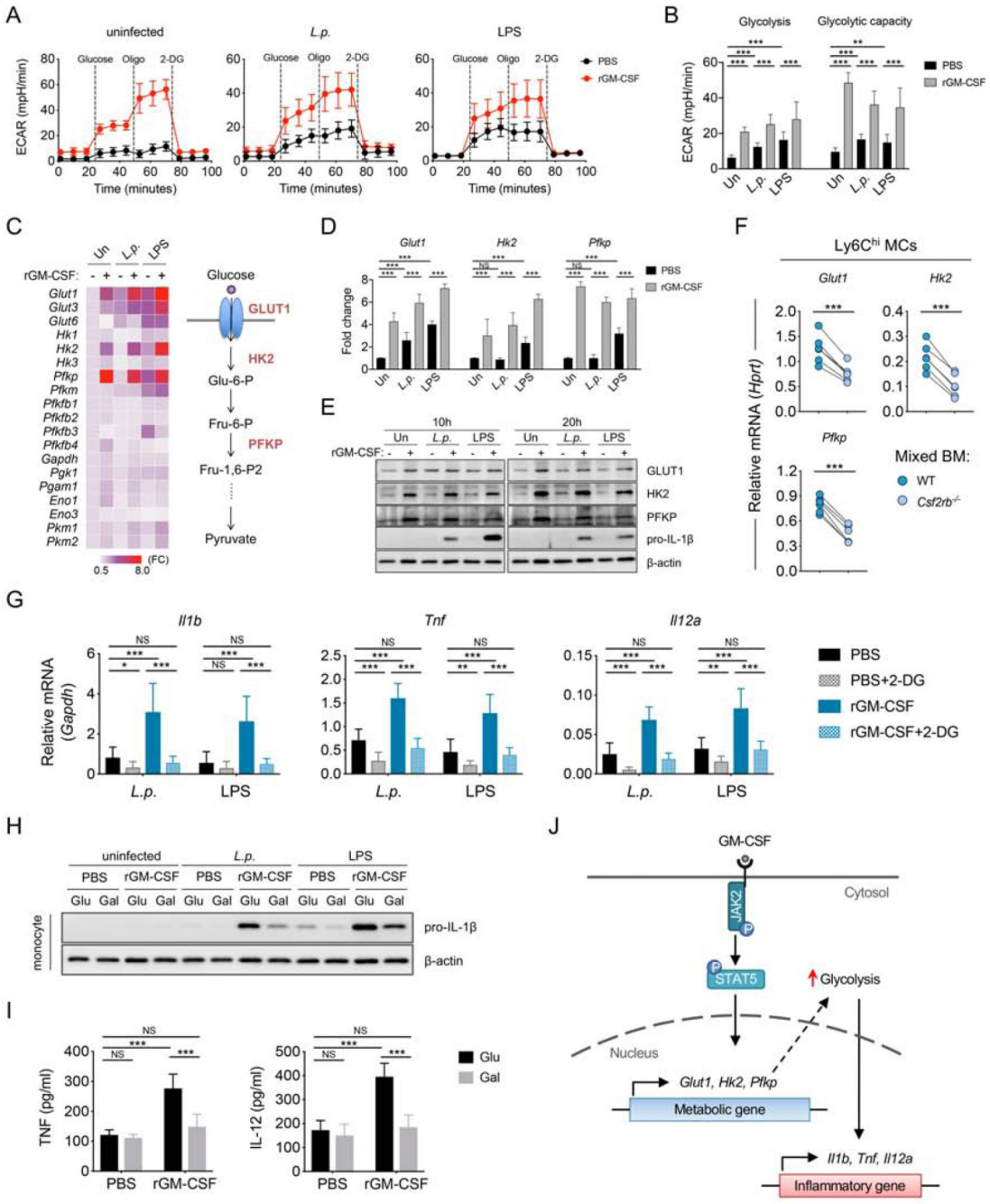

Figure 7. GM-CSF metabolically reprograms monocytes to undergo increased aerobic glycolysis, which supports cytokine production

(A and B) Seahorse analysis of real-time extracellular acidification rate (ECAR) (A), and statistical analysis of glycolysis and glycolytic capacity (B) of uninfected, *L.p.*-infected (MOI=5), or LPS-treated (10 ng/ml) MCs incubated with rGM-CSF (10 ng/ml) or PBS for 12 h before and after sequential treatment with glucose (10 mM), oligomycin (Oligo) (1 μ M), and 2-DG (50 mM).

(C and D) Heatmap depicting the fold-change in transcript levels of genes encoding glucose transporters and glycolytic enzymes in LPS- or *L.p.*-treated MCs incubated with rGM-CSF

(+) or PBS (−) for 10 h, relative to uninfected cells with PBS alone. Graphical model depicts an abbreviated version of the glycolytic pathway showing upregulated GLUT1, HK2 and PFKP expression following rGM-CSF treatment (C). Fold change of *Glut1*, *Hk2* and *Pfkp* transcript levels was quantified (D).

(E) Immunoblot analysis of GLUT1, HK2, PFKP, pro-IL-1β, and β-actin in the lysates of LPS or *L.p.*treated MCs incubated with rGM-CSF (+) or PBS (−) at 10 and 20 hpi.

(F) *Glut1*, *Hk2* and *Pfkp* transcript levels in WT and *Csf2rb*$^{-/-}$ Ly6C^{hi} MCs from the lungs of 50% WT/50% *Csf2rb*$^{-/-}$→WT mixed BM chimeras at 24 hpi. Each line represents the paired values of WT and *Csf2rb*$^{-/-}$ MCs from a given mouse.

(G) *Il1b*, *Tnf*, and *Il12a* transcript levels in LPS- or *L.p.*-treated MCs treated with 10 mM 2-DG or vehicle control in the presence of rGM-CSF or PBS at 6 hpi.

(H) Immunoblot analysis of pro-IL-1β and β-actin in the lysates of WT MCs incubated in media containing glucose (10 mM) or galactose (10 mM) that were then uninfected, infected with *L.p.* (MOI=5), or treated with LPS (10 ng/ml) in the presence of rGM-CSF or PBS for 10 hours.

(I) TNF and IL-12 levels in the supernatants of WT MCs incubated in media containing glucose or galactose, infected with *L.p.,* and treated with rGM-CSF or PBS at 10 hpi.

(J) Graphical model depicting that GM-CSF/JAK2/STAT5 signaling upregulates *Glut1*, *Hk2* and *Pfkp* expression and promotes aerobic glycolysis, which is critical for maximal inflammatory cytokine expression.

Data shown are the pooled results of three (A, B, G and I) or two (C and D) independent experiments with triplicate wells per condition in each experiment. Data shown in F are the pooled results of two independent experiments with 3 mice per experiment. Data shown in E and H are representative of two independent experiments. Data are represented as mean ± SD. NS, not significant; *p < 0.05; **p < 0.01; and ***p < 0.001 (unpaired t test for B and D; Wilcoxon matched-pairs signed rank test for F; one-way ANOVA with Turkey's multiple comparisons test for G; two-way ANOVA with Sidak's multiple comparisons test for I). See also Figure S6 and S7.

KEY RESOURCES TABLE

REAGENT or RESOURCE	SOURCE	IDENTIFIER
Antibodies		
Alexa Fluor 488 Rat anti-Mouse CD45 (clone 30-F11)	BioLegend	Cat#103122; RRID: AB_493531
PE Rat anti-Mouse CD45 (clone 30-F11)	BioLegend	Cat#103106; RRID: AB_312971
Pacific Blue Mouse anti-Mouse CD45.1 (clone A20)	BioLegend	Cat#110722; RRID: AB_492866
BV650 Mouse anti-Mouse CD45.2 (clone 104)	BioLegend	Cat#109835; RRID: AB_2563065
PE/Cy7 Rat anti-Mouse Ly6G (clone 1A8)	BioLegend	Cat#127618; RRID: AB_1877261
APC/Cy7 Rat anti-Mouse Ly6C (clone HK1.4)	BioLegend	Cat#128026; RRID: AB_10640120
BV785 Hamster anti-Mouse CD11c (clone N418)	BioLegend	Cat#117336; RRID: AB_2565268
Pacific Blue Rat anti-Mouse/Human CD11b (clone M1/70)	BioLegend	Cat#101224; RRID: AB_755986
Alexa Fluor 700 Rat anti-Mouse I-A/I-E (clone M5/114.15.2)	BioLegend	Cat#107621; RRID: AB_493726
PE-CF594 Rat anti-Mouse Siglec F (clone E50-2440)	BD Biosciences	Cat#562757; RRID: AB_2687994
PerCP/Cy5.5 Mouse anti-Mouse NK1.1 (clone PK136)	Thermo Fisher Scientific	Cat#45-5941-80; RRID: AB_914359
PE-CF594 Hamster anti-Mouse CD3e (clone 145-2C11)	BD Biosciences	Cat#562286; RRID: AB_11153307
APC/Cy7 Hamster anti-Mouse TCR β (clone H57-597)	BioLegend	Cat#109219; RRID: AB_893626
PE/Cy7 Hamster anti-Mouse TCR γ/δ (clone GL3)	BioLegend	Cat#118123; RRID: AB_11203530
Rat anti-Mouse CD16/CD32 (clone 93)	Thermo Fisher Scientific	Cat#14-0161-82; RRID: AB_467133
PerCP/Cy5.5 Rat anti-Mouse CD31 (clone MEC13.3)	BioLegend	Cat#102522; RRID: AB_2566761
PE/Cy7 Rat anti-Mouse EpCAM (clone G8.8)	Thermo Fisher Scientific	Cat#25-5791-80; RRID: AB_1724047
APC/Cy7 Hamster anti-Mouse T1a (clone 8.1.1)	BioLegend	Cat#127418; RRID: AB_2629804
Pacific Blue Rat anti-Human/Mouse CD49f (clone GoH3)	BioLegend	Cat#313619; RRID: AB_2128022
PE-CF594 Rat anti-Mouse Sca-1 (clone D7)	BD Biosciences	Cat#562730; RRID: AB_2737751
PE Hamster anti-Mouse IL-1α (clone ALF-161)	Thermo Fisher Scientific	Cat#12-7011-82; RRID: AB_466144
APC Rat anti-Mouse IL-1β (clone NJTEN3)	Thermo Fisher Scientific	Cat#17-7114-80; RRID: AB_10670739
APC Rat anti-Mouse TNFα (clone MP6-XT22)	Thermo Fisher Scientific	Cat#17-7321-81; RRID: AB_469507
PE Rat anti-Mouse IL-12 p40 (clone C15.6)	BioLegend	Cat#505204; RRID: AB_315368
Biotin Rat anti-Mouse GM-CSF (clone MP1-31G6)	BioLegend	Cat#505501; RRID: AB_315385
PE Hamster IgG Isotype (clone eBio299Arm)	Thermo Fisher Scientific	Cat#12-4888-81; RRID: AB_470073
APC Rat IgG1 κ Isotype (clone eBRG1)	Thermo Fisher Scientific	Cat#17-4301-82; RRID: AB_470178
PE Rat IgG1 κ Isotype (clone RTK2071)	BioLegend	Cat#400407; RRID: AB_326513
Biotin Rat IgG1 κ Isotype (clone RTK2071)	BioLegend	Cat#400403; RRID: AB_326509
Rat anti-Mouse IL-12 p40/p70 (clone C15.6)	BD Biosciences	Cat#551219; RRID: AB_394097
Biotin Rat anti-Mouse IL-12 p40/p70 (clone C17.8)	BD Biosciences	Cat#554476; RRID: AB_395419
Mouse anti-Mouse IL-1β (clone 3A6)	Cell Signaling Technology	Cat#12242; RRID: AB_2715503
Rabbit anti-Mouse/Human GLUT1 (polyclonal Ab)	Thermo Fisher Scientific	Cat#PA1-46152; RRID: AB_2302087
Rabbit anti-Mouse/Human HK2 (clone C64G5)	Cell Signaling Technology	Cat#2867; RRID: AB_2232946
Rabbit anti-Mouse/Human PFKP (polyclonal Ab)	Thermo Fisher Scientific	Cat#PA5-28673; RRID: AB_2546149
Rabbit anti-Mouse/Human β-actin (polyclonal Ab)	Cell Signaling Technology	Cat#4967; RRID: AB_330288

REAGENT or RESOURCE	SOURCE	IDENTIFIER
HRP-linked Horse anti-Mouse IgG	Cell Signaling Technology	Cat#7076; RRID: AB_330924
HRP-linked Goat anti-Rabbit IgG	Cell Signaling Technology	Cat#7074; RRID: AB_2099233
InVivoMAb Rat anti-Mouse GM-CSF (clone MP1-22E9)	Bio X Cell	Cat#BE0259; RRID: AB_2687738
InVivoMAb Rat anti-Mouse IgG2a κ Isotype (clone 2A3)	Bio X Cell	Cat#BE0089; RRID: AB_1107769
Bacterial and Virus Strains		
Legionella pneumophila Lp02 Δ*flaA*	Ren et al., 2006	N/A
Legionella pneumophila Lp02 Δ*dotA*	Berger and Isberg, 1993	N/A
Legionella pneumophila JR32 Δ*flaA*	Ren et al., 2006; Sadosky et al., 1993	N/A
Chemicals, Peptides, and Recombinant Proteins		
LPS from *E. coli* K12	InvivoGen	Cat#tlrl-peklps
Streptavidin APC Conjugate	Thermo Fisher Scientific	Cat#17-4317-82
GolgiPlug™ Brefeldin A	BD Biosciences	Cat#555029
GolgiStop™ Monensin	BD Biosciences	Cat#554715
JAK2 Inhibitor (NVP-BSK805 2HCl)	Selleck Chemicals	Cat#S2686
STAT5 Inhibitor (Pimozide)	Millipore Sigma	Cat#573110
Halt™ Protease and Phosphatase Inhibitor Cocktail	Thermo Fisher Scientific	Cat#78440
SuperScript™ II Reverse Transcriptase	Thermo Fisher Scientific	Cat#18064014
SsoFast™ EvaGreen Supermix with Low ROX	Bio-Rad	Cat#1725212
Collagenase IV	Worthington Biochemical	Cat#LS004188
Cytofix/Cytoperm™ Fixation and Permeabilization Solution	BD Biosciences	Cat#554722
Perm/Wash Buffer	BD Biosciences	Cat#554723
SuperSignal™ Substrates (Dura/Femto)	Thermo Fisher Scientific	Cat#34076/34095
Dispase	Worthington Biochemical	Cat#LS02104
DNase I	Thermo Fisher Scientific	Cat#4716728001
Tamoxifen	Sigma-Aldrich	Cat#T5648
Corn Oil	Sigma-Aldrich	Cat#C8267
2-Deoxy-D-glucose (2-DG)	Sigma-Aldrich	Cat#D6134
Glucose	Sigma-Aldrich	Cat#G8769
Galactose	Sigma-Aldrich	Cat#G5388
Dialyzed FBS	Thermo Fisher Scientific	Cat#A3382001
RPMI without Glucose	Thermo Fisher Scientific	Cat#11879020
Seahorse XF Base Medium	Agilent Technology	Cat#102353-100
Rock Inhibitor (Y-27632)	Selleck Chemicals	Cat#S1049
Charcoal-Stripped FBS	Sigma-Aldrich	Cat#F6765
Low Melting Temperature SeaPlaque™ Agarose	Lonza	Cat#50100
Matrigel® Growth Factor Reduced Basement Membrane Matrix	Corning	Cat#354230
Recombinant Mouse IL-1α	BioLegend	Cat#575002
Recombinant Mouse IL-1β	BioLegend	Cat#575102
Recombinant Mouse GM-CSF	BioLegend	Cat#576304

REAGENT or RESOURCE	SOURCE	IDENTIFIER
Recombinant Mouse IL-12 p70	PeproTech	Cat#210-12
Recombinant Human KGF	PeproTech	Cat#100-19
Critical Commercial Assays		
Monocyte Isolation Kit	Miltenyi Biotec	Cat#130-100-629
Mouse Interferon-Gamma ELISA Set	BD Biosciences	Cat#555138
Mouse IL-1α ELISA MAX Standard Kit	BioLegend	Cat#433403
Mouse IL-1β ELISA MAX Standard Kit	BioLegend	Cat#432603
Mouse TNFα ELISA MAX Standard Kit	BioLegend	Cat#430903
Mouse GM-CSF ELISA MAX Standard Kit	BioLegend	Cat#432201
Mouse IL-6 ELISA MAX Standard Kit	BioLegend	Cat#431303
Mouse Cytokine/Chemokine Magnetic Bead Panel - Premixed 32 Plex - Assay Kit	Millipore Sigma	Cat#MCYTMAG-70K-PX32
RNeasy Mini Kit	Qiagen	Cat#74106
Zombie Yellow™ Fixable Viability Kit	BioLegend	Cat#423104
CellROX™ Deep Red Flow Cytometry Assay Kit	Thermo Fisher Scientific	Cat#C10491
Seahorse XFe96 FluxPak Mini Kit	Agilent Technology	Cat#102601-100
Seahorse XF Glycolysis Stress Test Kit	Agilent Technology	Cat#103020-100
Seahorse XF Cell Mito Stress Test Kit	Agilent Technology	Cat#103015-100
Experimental Models: Cell Lines		
Mouse: C57BL/6J BMDM	This paper	N/A
Mouse: *Csf2*$^{-/-}$ BMDM	This paper	N/A
Mouse: C57BL/6J monocyte	This paper	N/A
Mouse: C57BL/6J AECII	This paper	N/A
Mouse: *Il1r1*$^{-/-}$ AECII	This paper	N/A
Experimental Models: Organisms/Strains		
Mouse: C57BL/6J	Jackson Laboratory	RRID: IMSR_JAX:000664
Mouse: B6.SJL- *Ptprc*^{a} *Pepc*^{b}/BoyJ	Jackson Laboratory	RRID: IMSR_JAX:002014
Mouse: *Il1a*$^{-/-}$	Horai et al., 1998	N/A
Mouse: *Il1b*$^{-/-}$	Horai et al., 1998	N/A
Mouse: *Il1r1*$^{-/-}$: B6.129S7-*Il1r1*^{tm1Imx}/J	Jackson Laboratory	RRID: IMSR_JAX:003245
Mouse: *Csf2*$^{-/-}$: B6.129S-*Csf2*^{tm1Mlg}/J	Jackson Laboratory	RRID: IMSR_JAX:026812
Mouse: *Csf2rb*$^{-/-}$: B6.129S1-*Csf2rb*^{tm1Cgb}/J	Jackson Laboratory	RRID: IMSR_JAX:005940
Mouse: *Il1r1*$^{fl/fl}$: B6.129(Cg)-*Il1r1*$^{tm1.1Rbl}$/J	Jackson Laboratory	RRID: IMSR_JAX:028398
Mouse: *Il1r1*$^{r/r}$: C57BL/6N-*Il1r1*^{tm1Quan}/J	Jackson Laboratory	RRID: IMSR_JAX:024101
Mouse: *Spc-creER*^{T2}: B6.129S-*Sftpc*$^{tm1(cre/ERT2)Blh}$/J	Jackson Laboratory	RRID: IMSR_JAX:028054
Mouse: *Il1r1*$^{fl/fl}$;*Spc-creER*^{T2}	This paper	N/A
Mouse: *Il1r1*$^{r/r}$;*Spc-creER*^{T2}	This paper	N/A
Oligonucleotides		
Primers for qRT-PCR, see Table S1	See Table S1	N/A

REAGENT or RESOURCE	SOURCE	IDENTIFIER
Software and Algorithms		
GraphPad Prism v7.0 and v8.0	GraphPad	http://www.graphpad.com
FlowJo v10.3	FlowJo, LLC	http://www.flowjo.com
Wave v2.4	Agilent Technology	http://www.agilent.com